Contents lists available at ScienceDirect

Ecological Informatics
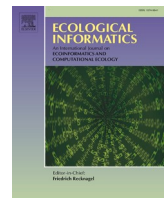
Long-term phosphorus mass-balance of Lake Erie (Canada-USA) reveals a major contribution of in-lake phosphorus loading

Serghei Anatolii Bocaniov [a,c,*], Donald Scavia [b], Philippe Van Cappellen [a,c]

[a] *Ecohydrology Research Group, Department of Earth and Environmental Sciences, University of Waterloo, Waterloo, ON N2L 3G1, Canada*
[b] *School for Environment and Sustainability, University of Michigan, 440 Church St., Ann Arbor, MI 48104, USA*
[c] *Water Institute, University of Waterloo, Waterloo, ON N2L 3G1, Canada*

ARTICLE INFO

ABSTRACT

While early efforts to reduce external phosphorus (P) loads to Lake Erie eliminated the worst eutrophication symptoms in the 1970s and 1980s, the observed intensification of these symptoms in recent decades is difficult to explain by changes in the external P loading alone. We hypothesized that, in addition to external inputs, in-lake processes that release P to the water column may be contributing to the re-eutrophication of Lake Erie. Directly measuring these internal inputs is challenging and their scaling up to the entire lake system remains fraught with uncertainty. To constrain the magnitude of the net P input associated with in-lake processes, we generated a long-term annual total P (TP) budget for the Lake St. Clair–Lake Erie system, averaged over a 14-year period, from 2003 to 2016. The budget shows that the TP output from the system substantially exceeds the sum of the external TP inputs. To balance the budget, we estimate that in-lake processes add a net internal TP load of 3783 metric tons per year (MTA) to the water column. In comparison, the mean yearly external TP load to the Lake St. Clair–Lake Erie system is 11,703 MTA. Thus, overall, in-lake processes account for about a quarter of the total (external plus internal) TP input. The internal input is not evenly distributed among the system's basins, however, with Lake St. Clair and Lake Erie's western, central, and eastern basins receiving 6, 13, 21 and 60% of the total internal P input, respectively. Our results highlight the importance of accounting for the internal P loading in nutrient cycling modeling and load reduction strategies for large lake systems.

1. Introduction

The primary driver of cultural eutrophication is excess nutrient inputs from human activities. Management strategies aimed at mitigating the negative effects of lake eutrophication therefore focus on reducing external nutrient loads, with particular attention on phosphorus (P), the key macronutrient (co-)limiting primary production in aquatic ecosystems. Yet, many of these systems show increasing signs of eutrophication, even under stable or even reduced external loads. Examples range from small ponds to the coastal ocean (Fu et al., 2018), including estuaries and coastal bays (e.g., Chesapeake Bay: Najjar et al., 2010), enclosed and semi-enclosed seas (e.g., Baltic Sea: Munkes, 2005; Vahtera et al., 2007; Meier et al., 2011; Stigebrandt and Andersson, 2020), and lakes, such as Lake Winnipeg (Matisoff et al., 2017; Nürnberg and LaZerte, 2016), Lake of the Woods (Edlund et al., 2017; James, 2017), Lake Chaohu (Yang et al., 2020), and Lake Erie (Matisoff et al., 2016;

Scavia et al., 2014).

While early efforts to reduce external P loads to Lake Erie (IJC (International Joint Commission), 1978) initially eliminated the worst eutrophication symptoms, the lake has shown signs of re-eutrophication beginning in the late 1990s. In particular, since that time there have been more frequent and more severe cyanobacterial harmful algal blooms (HABs), expanded regions of bottom-water hypoxia, outbreaks of nuisance benthic green algae (e.g., *Cladophora glomerata*), and increased total phosphorus (TP) concentrations in the western and central basins (Rucinski et al., 2014; Scavia et al., 2014; Watson et al., 2016) compared to the 1980s and early to mid 1990s.

In addition to external P loads that are driven by on-land human activities and modulated by watershed hydrology and airshed transport, in-lake processes may also release P to the water column. This internally sourced P can be assimilated into the food web and contribute to eutrophication. In-lake mechanisms of P mobilization may be enhanced

---

* Corresponding author at: Ecohydrology Research Group, Department of Earth and Environmental Sciences, University of Waterloo, Waterloo, ON N2L 3G1, Canada.

E-mail address: sbocaniov@uwaterloo.ca (S.A. Bocaniov).

by rising water temperature (Boström et al., 1982; Gomez et al., 1998; Jeppesen et al., 1997), photosynthetically driven pH increases (Sabur et al., 2021; Søndergaard et al., 2003; Welch and Cooke, 1995) in shallow environments characterized by dense cyanobacterial blooms (Chen et al., 2014, 2018; Zepernick et al., 2021), hypolimnetic hypoxia and anoxia (Nürnberg et al., 2019; Orihel et al., 2017; Welch and Cooke, 1995), salinization (Radosavljevic et al., 2022), and coastal sediment resuspension and shoreline erosion (Eadie et al., 1990, 2008; McKinney et al., 2019; Scavia et al., 2019a, 2019b, 2020). Despite growing evidence that these mechanisms can mobilize significant amounts of P (e.g., Nürnberg and LaZerte, 2016; Scavia et al., 2020), quantifying internal P loads in large lakes is difficult because the underlying mechanisms are generally highly dynamic in time and space.

Several studies have reported large internal P fluxes in Lake Erie (Matisoff et al., 2016; Paytan et al., 2017; Nürnberg et al., 2019; Gibbons and Bridgeman, 2020; Wang et al., 2021; Anderson et al., 2021; see Table A1: Tables, Figures and Appendices indexed with letters "A" and "B" can be found in corresponding Supporting Material A and B). For example, estimates for Lake Erie's central basin as high as 11,000 metric tons per year (MTA) have been proposed (Anderson et al., 2021). However, the existing measurements cover limited spatial and temporal

scales, and may not be representative of the integrated long-term and basin-wide contribution of in-lake mobilization processes to the water column TP budget. While there is a general consensus that the re-eutrophication of the western basin of Lake Erie, including the recurrent HABs, is primarily driven by the external P loads, internal P loading may still play a role in modulating algal productivity, especially in years when the external P loading is relatively low (Matisoff et al., 2016). The magnitude of the internal P loading in the western basin, however, remains poorly constrained.

To assess the magnitudes of internal total P (TP) loads and compare them to external inputs, we constructed a 14-year average annual TP budget for Lake Erie. (Note: TP comprises all the P in a bulk water sample, including dissolved and particulate P, and both inorganic and organic forms of P). A multi-year averaging helps delineating the main features of elemental budgets of large lakes with relatively long water residence times (~2.8 years for Lake Erie; Bolsenga and Herdendorf, 1993). The difference between all external P inputs and all P outputs (including P accumulation in bottom sediments) then provides an estimate of the internal TP input (Orihel et al., 2017). The only assumption in this mass-balance approach is that the long-term TP budget is closed. It is important to note that, in and of itself, the approach does not
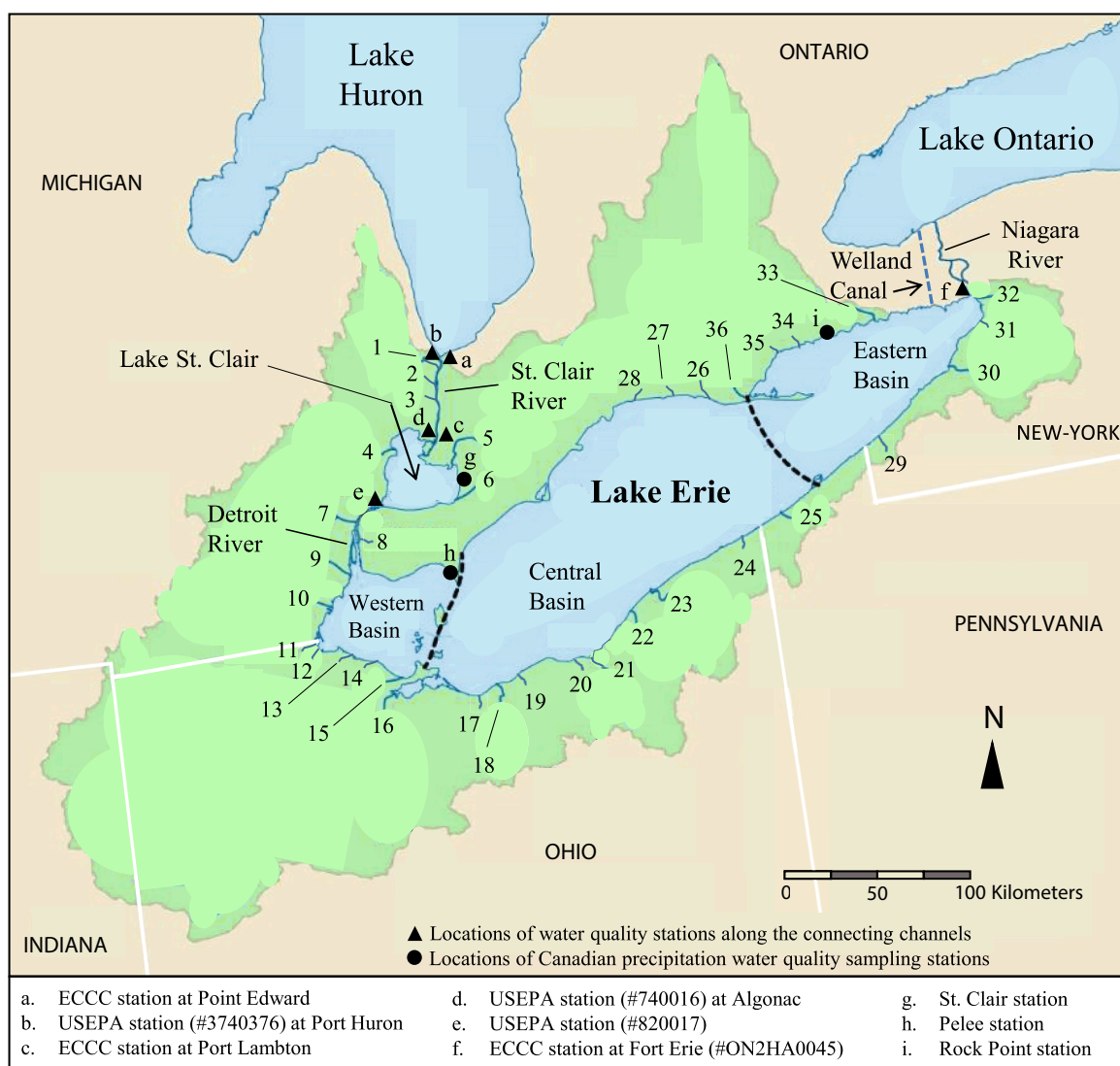
Fig. 1. Map of the Lake St. Clair-Lake Erie system with selected 36 major lake tributaries, locations of water quality monitoring stations along the connecting channels, and stations where precipitation is collected for water quality purposes. Tributaries are indicated by numbers corresponding to their names in Table 5. Area in green indicates the boundaries of the watershed area. (For interpretation of the references to colour in this figure legend, the reader is referred to the web version of this article.)

identify which in-lake processes are responsible for the internal TP input. We apply the approach to Lake Erie because it has a well-documented history of cultural eutrophication and has extensive data on the external P inputs and in-lake water quality.

Lake Erie has three distinct basins (Fig. 1) with variable trophic states, morphometric properties, and thermal and mixing regimes, making them representative of a broader range of systems. Comparison of the budget calculations for the three basins may therefore yield insights into the role of internal P loading that are transferable across a range of large lake systems. Note that we include Lake St. Clair in our analysis because it is an integral part of Lake Erie's watershed (Bolsenga and Herdendorf, 1993; Chapra et al., 2016) and represents a significant modifier of the P fluxes from Lake Huron to Lake Erie (Bocaniov et al., 2019; Scavia et al., 2019a, 2019b).

2. Methods and data sources

2.1. Study region

The Lake St. Clair–Lake Erie System is part of the Laurentian Great Lakes–St. Lawrence River drainage system in the upper mid-west of North America. It is located between Lake Huron and Lake Ontario (Fig. 1) and consists of the Huron-Erie Corridor (HEC: St. Clair River, Lake St. Clair, and Detroit River) and Lake Erie proper. In addition to its own watershed, HEC receives water and accompanying chemical loads from Lake Huron. Lake St. Clair is a relatively large, shallow, oligo-mesotrophic, polymictic lake (mean depth = 3.8 m; maximum natural depth = 6.4 m; Bocaniov and Scavia, 2018; Bocaniov et al., 2019). It is connected to Lake Huron via the St. Clair River and flows into the Detroit River that, in turn, flows into the western basin of Lake Erie. Note that the St. Clair River and Detroit River are connecting channels rather than actual rivers (Bolsenga and Herdendorf, 1993).

Lake Erie itself is a large, relatively shallow lake separated topographically into three basins with distinct morphometric characteristics, mixing regimes, and trophic conditions (Bolsenga and Herdendorf, 1993). The western and eastern basins are the most and least productive, respectively. The western basin is the shallowest (mean and maximum depths: 7.3 and 19 m), characterized by a prevailing polymictic mixing regime, but with short episodes of hypoxia in summer (Jabbari et al., 2019), and dense cyanobacterial blooms towards the end of summer and early fall (Sayers et al., 2019). It is separated from the central basin by a chain of rocky islands and shoals (Fig. 1). The central basin is dimictic (mean and maximum depths: 18.3 and 26 m) and deep enough to stratify vertically from mid-June to mid-late October with an hypolimnion susceptible to seasonal hypoxia. The eastern basin is the deepest (mean and maximum depths: 24 and 63 m) with the second largest volume and surface area. The major outflow from Lake Erie is through the Niagara River, the channel connecting Lake Erie to Lake Ontario, and the Well-and Canal (Fig. 1). The latter was built to bypass the Niagara Falls and provide a deep draft navigation connection between the two lakes.

2.2. Lake segmentation and watershed delineation

The Lake St. Clair–Lake Erie system was divided into the following segments along with their corresponding watersheds: St. Clair River, Lake St. Clair, and Detroit River, plus Lake Erie's western, central, and eastern basins. Delineation of the Canadian sub-watersheds (Table A2 and Fig. A1) was based on the tertiary and quaternary sub-watersheds identified in the Ontario Watershed Boundaries dataset (ODC, 2019). Delineation of the United States sub-watersheds (Table A3; Fig. A1) was based on the U.S. Geological Survey (USGS) 6-digit and 8-digit hydrologic unit codes (HUC6, HUC8) in the U.S. Watershed Boundary Dataset (WBD, 2019). Together, this yielded 67 Canadian and 28 U.S. sub-watersheds (Tables A2 & A3) that include not only the major river tributaries flowing into the St. Clair River, Lake St. Clair, the Detroit River, and Lake Erie, but also the smaller, nearshore watersheds with direct

drainage to the different lake segments.

2.3. Long-term budgets: Approach

We constructed long-term, post-2000 water and TP mass balances (Table 1: Eqs. 1–6 for water and 7–12 for TP; see Table 2 for definitions of the symbols in the equations) for the four major segments of the Lake St. Clair–Lake Erie system by averaging data of 14 water years, from October 1, 2002, to September 30, 2016. For each segment, the water cycle was assumed to be closed, with inflows and over-lake precipitation equal to outflows and evaporation, plus or minus the change in water volume. The (unknown) in-lake TP loading fluxes (L_i) were obtained for each segment by solving Eqs. 8 and 10–12 (Table 1) assuming steady state conditions ($dp/dt = 0$, with p representing the TP concentration). In preliminary work, we performed non-steady state calculations (i.e., $dp/dt \neq 0$) where we incorporated the observed temporal trends in TP concentration over the study period. These calculations, however, produced results very close to those of the steady state calculations (Table A1). Data sources for the water and TP balances are provided in Tables A4 to A9. The following two sub-sections describe how the various terms in the water and TP mass balance equations were estimated. Further details can be found in Appendices A2 to A7.

Table 1

Mass balance equations for calculating the mean annual water and TP mass balances (with eqs. 7–12 modified after Chapra et al., 2016) averaged over the 2003–2016 period. See Table 2 for the definitions of the symbols.

Segment	Equation	Eq. #
	Segment-specific water mass budgets:	
St. Clair River	$Q_{scr,ds} = Q_{scr,us} + R_{scr}$	(1)
Lake St. Clair	$Y_s + R_s + Q_{scr,ds} + Q_{HWTP} + Q_s^{gw} = E_s + Q_{dr,us} + \Delta V_s + CU_s$	(2)
Detroit River	$Q_{dr,ds} = Q_{dr,us} + R_{dr}$	(3)
Western Basin (Lake Erie)	$Y_w + R_w + Q_{dr,ds} + Q_w^{gw} = E_w + Q_w + \Delta V_w + CU_w$	(4)
Central Basin (Lake Erie)	$Y_c + R_c + Q_w + Q_c^{gw} = E_c + Q_c + \Delta V_c + CU_c$	(5)
Eastern Basin (Lake Erie)	$Y_e + R_e + Q_c + Q_e^{gw} = E_e + Q_{nr,us} + Q_{wc,us} + \Delta V_e + CU_e$	(6)
	Segment-specific phosphorus mass budgets:	
St. Clair River	$W_{scr}^T = Q_{scr,us} \bullet p_{LH} + W_{scr}^R = Q_{dr,ds} \bullet p_{dr,ds}$	(7)
Lake St. Clair	$V_s \frac{dp_s}{dt} = W_{scr}^T + W_s^R - Q_{dr,us} \bullet p_s - v_s \bullet A_s \bullet p_s - \Delta V_s \bullet p_s - CU_s \bullet p_s + Y_s \bullet p_s^{PR} \bullet k + Q_s^{gw} \bullet p^{gw} + L_s$	(8)
Detroit River	$W_{dr}^T = Q_{dr,us} \bullet p_s + W_{dr}^R = Q_{dr,ds} \bullet p_{dr,ds}$	(9)
Western Basin (Lake Erie)	$V_w \frac{dp_w}{dt} = W_{dr}^T + W_w^R - Q_w \bullet p_w + E'_{w/c}(p_c - p_w) - v_w \bullet A_w \bullet p_w - \Delta V_w \bullet p_w - CU_w \bullet p_w + Y_{LE} \bullet p_{LE}^{PR} \bullet k \bullet a_w + Q_w^{gw} \bullet p^{gw} + L_w$	(10)
Central Basin (Lake Erie)	$V_c \frac{dp_c}{dt} = Q_w \bullet p_w + W_c^R - Q_c \bullet p_c + E'_{w/c}(p_w - p_c) + E'_{c/e}(p_e - p_c) - v_c \bullet A_c \bullet p_c - \Delta V_c \bullet p_c - CU_c \bullet p_c + Y_{LE} \bullet p_{LE}^{PR} \bullet k \bullet a_c + Q_c^{gw} \bullet p^{gw} + L_c$	(11)
Eastern Basin (Lake Erie)	$V_e \frac{dp_e}{dt} = Q_c \bullet p_c + W_e^R - (Q_{nr} + Q_{wc}) \bullet p_{nr} + E'_{c/e} \bullet (p_c - p_e) - v_e \bullet A_e \bullet p_e - \Delta V_e \bullet p_e - CU_e \bullet p_e + Y_{LE} \bullet p_{LE}^{PR} \bullet k \bullet a_e + Q_e^{gw} \bullet p^{gw} + L_e$	(12)

Note: Eqs. 8 and 10 to 12 can be solved at steady state (i.e., all $dp/dt = 0$) and at non-steady state ($dp/dt \neq 0$). In both cases, these equations form linear algebraic systems with only one unknown, that is, the internal load (L).

Table 2
Definitions of abbreviations, variables, and parameters in the water and phosphorus mass balance equations shown in Table 1.

#	Term	Explanation
1	TP	Total phosphorus
2	s, w, c, e	Abbreviations for Lake St. Clair (s), Western Basin (w), Central Basin (c), and Eastern Basin (e)
3	scr, dr, nr	Abbreviations for the St. Clair River (scr), Detroit River (dr), and Niagara River (nr)
4	gw, wc, LH, LE	Abbreviations for ground water (gw), Welland Canal (wc), Lake Huron (LH), and Lake Erie (LE)
5	$HWTP$	Huron water treatment plant
6	us, ds	Upstream location (us), downstream location (ds)
7	Y_i, E_i	Over-water precipitation (Y_i) and over-water evaporation (E_i) for segment i (km^3 yr^{-1})
8	R_i	Total watershed outflow reaching segment i (km^3 yr^{-1})
9	i	Segment index
10	Q_i	Advective outflow from segment i (km^3 yr^{-1})
11	Q_i^{gw}	Ground water discharge into segment i (km^3 yr^{-1})
12	W_i^T, W_i^R	Direct mass loading of total phosphorus (MTA) to segment i with subscript T representing inflow plus total watershed inputs, and subscript R representing total watershed inputs
13	A_i	Surface area (km^2) for segment i: $A_s = 1114$; $A_w = 3284$; $A_c = 16{,}138$; $A_e = 6235$
14	$E'_{w/c}, E'_{c/e}$	Bulk dispersion coefficient for turbulent transport (km^3 yr^{-1}) between Lake Erie basins (Chapra et al., 2016): $E'_{w/c} = 22.1$ and $E'_{c/e} = 197.5$
15	V_b	Volume of segment i (km^3)
16	ΔV_i	Rate of change in volume (ΔV_i) obtained from the difference in volume i between time t and $t = 0$ for segment i (km^3 yr^{-1})
17	p_i	TP concentration (µg L^{-1} or mg m^{-3}) in segment i
18	p^{gw}	Median TP concentration in groundwater: $p^{gw} = 20$ µg L^{-1} (Table 9)
19	p_i^{PR}	Estimated volume weighted mean concentration of TP in precipitation for segment i (Appendix A5; Table A10)
20	CU_i	Consumptive water use in segment i (km^3 yr^{-1})
21	v_i	Apparent settling velocity of TP (m yr^{-1}) in segment i: $v_s = 50$; $v_w = 50$; $v_c = 30$; $v_e = 32$ (Chapra et al., 2016)
22	L_i	Internal TP load (MTA) required to balance inputs and outputs for segment i
23	k	Coefficient to compute total (wet and dry) TP deposition from wet deposition; $k = 3.45$ (Anderson and Downing, 2006)
24	a_i	Area of segment i as a proportion of total Lake Erie surface area: $a_w = 0.128$; $a_c = 0.629$; $a_e = 0.243$ (Table 4)
25	MTA	Metric tons per year

2.4. Water budgets

The annual volumes and water inputs and outputs for all the lake segments were estimated for each of the 14 water years, and then averaged to construct the average water budgets for Lake St. Clair and Lake Erie. Where required, minor adjustments were made to close the water budgets (Appendix A3). Next, the closed water budget of Lake Erie was further divided into the three, western, central, and eastern basin-specific water budgets (Eqs. 4–6; Table 1).

Annual volumes and surface areas of the Lake St. Clair–Lake Erie segments were derived from the lake bathymetry (NOAA, 2020a) and water levels (Table A5). The latter were estimated from the mean daily water levels measured at multiple locations with gauges operated by Canada's Department of Fisheries and Oceans (DFO, 2020) and the United States National Oceanic and Atmospheric Administration (NOAA, 2020b). Annual net changes in storage of Lake St. Clair and Lake Erie were calculated as the product of the measured changes in lake stage times the lake surface area. For the St. Clair River and Detroit River connecting channels, the annual volume was calculated as the product of the mean annual flow and the reported literature value of the water storage capacity (0.88 days for the St. Clair River, Griffiths et al., 1991; 0.83 days for the Detroit River, Derecki, 1984). The approximation of a constant storage capacity for the connecting channels introduced negligible errors in the much larger Lake St. Clair and Lake Erie water budgets.

Monthly over-lake precipitation and evaporation data were obtained from the NOAA Great Lakes Environmental Research Laboratory Hydrologic Data base (GLERL, 2020a). For Lake Erie's three basins, precipitation and evaporation rates were prorated using the ratios of the basin surface areas to the total lake area. Daily flow rates for the major tributaries were downloaded from the USGS National Water Information System (USGS, 2019) and the National Water Data Archive HYDAT (HYDAT, 2020) for sites in the United States and Canada, respectively (Tables A4 & A5). For rivers with multiple flow gauges, area-weighted estimates of flow at the downstream confluence were used. The flow data were scaled up to the corresponding entire sub-watershed areas to account for the unmonitored area runoff (Tables A2 & A3).

The annual direct groundwater inflow to Lake Erie (11.9 m^3 s^{-1}) was derived from integrated surface water-groundwater modeling results (Xu et al., 2021). To estimate the groundwater flux to an individual lake segment, the total groundwater inflow was prorated using the ratio of the segment's water surface area to the total water surface assuming 0.5 m^3 s^{-1} for Lake St. Clair and 11.5 m^3 s^{-1} for Lake Erie. For Lake Erie this yielded 1.5, 7.2 and 2.8 m^3 s^{-1} for the western, central, and eastern basin, respectively. The two major water diversions considered were the Welland Canal (Fig. 1), which moves water from Lake Erie's eastern basin to Lake Ontario, and the Detroit public water intake, which transfers Lake Huron water to the water supply system that subsequently returns it to Lake St. Clair (average daily flow of 7.0 m^3 s^{-1}, 2003 to 2015 data: DWSD, 2019). Consumptive water usage was obtained from the Great Lakes Regional Water Use Database (GLC, 2019).

2.5. Total phosphorus (TP) budgets

For each lake and connecting channel segment, annual TP water column standing stocks, inputs, and outputs were estimated and then averaged over the 14 water years. The estimates combined water column volumes and water fluxes from the water budgets with mean TP concentrations in water columns, tributaries, and other input and output pathways. To estimate the removal of TP from the water column by sediment deposition at the lake floor, we used the apparent settling velocities reported by Chapra et al. (2016). These authors provide a detailed discussion of these rates, including their spatial and historical (pre-vs. post-1990) variability, and the possible reasons for their variability. Inter-basin TP exchanges in Lake Erie were separated between advective and dispersive fluxes, where the latter fluxes were estimated based on average annual TP concentration differences between adjacent basins and reported bulk dispersion coefficients for turbulent transport between basins (Tables 1 and 2). For Lake Erie, the TP mass balance was first developed for the entire lake and then the estimated inter-basin P exchanges were used to split the whole-lake TP budget into the three basin-specific budgets.

Lake Erie TP concentrations were extracted from the U.S. Environmental Protection Agency (USEPA) Great Lakes National Program Office (GLNPO, 2020), which conducts two lake-wide offshore monitoring cruises each year to characterize both the well-mixed spring (early April) and stratified summer (August) conditions, with 6, 10 and 4 sampling stations in the western, central, and eastern basins, respectively. Similar to previous studies (e.g., Chapra et al., 2016), representative annual basin-specific concentrations were obtained by averaging the spring and summer median values to make the results less sensitive to the outliers. Because there are no systematic in-lake monitoring data of TP concentrations in Lake St. Clair, the TP concentrations measured in the lake outflow (USEPA station #820017; Fig. 1) were used to represent in-lake concentrations. This is justified by Lake St. Clair's short hydraulic residence time (~10 days; Bocaniov and Scavia, 2018).

For any given water year, the TP standing stock in each of Lake Erie's basins was estimated as the product of the basin water volume times the mean basin-specific TP concentration for that year. For Lake St. Clair, the annual TP standing stocks were calculated as the lake's annual water volume times the mean annual concentration in the lake' outflow to the

Detroit River. Annual standing stocks of TP of the St. Clair River and Detroit River channels were calculated by dividing the mean annual TP load to the channel by the flushing rate, where the latter is equal to the ratio of the mean annual water discharge divided by the channel volume. The TP removal via consumptive water use was calculated as the annual rate of consumptive water use multiplied by the basin-specific average annual TP concentration. TP loss due to changes in lake storage was estimated as the annual rate of change of the volume multiplied by the corresponding basin-specific average annual TP concentration.

Data on TP concentrations in inflows and outflows were extracted from multiple sources, including the United States Water Quality Portal (WQP, 2019), National Center for Water Quality Research at Heidelberg University, Ohio (NCWQR, 2020), Michigan Department of Environmental Quality (MDEQ), Provincial (Stream) Water Quality Monitoring Network (PWQMN, 2019), Ontario Provincial Groundwater Monitoring Network (PGMN, 2022), Great Lakes Intake Program (GLIP, 2019) managed by the Ontario Ministry of the Environment, Conservation and Parks (MECP), and Environment and Climate Change Canada (ECCC).

All tributary TP loads were estimated with the Weighted Regression on Time, Discharge, and Season (WRTDS) method (Hirsch et al., 2010) using reported concentrations and flow data. The WRTDS method, however, could not be applied to the three connecting channels (St. Clair River, Detroit River, and Niagara River) because the TP concentrations and discharge flows are not correlated. Following Scavia et al. (2019a, 2019b), we therefore used the Generalized Additive Model (GAM, Wood, 2011, 2017) to approximate daily TP concentrations as a function of time, with the smoothing parameters selected with the Restricted Maximum Likelihood (REML) method. The estimated daily TP concentrations and standard errors were multiplied by the corresponding daily discharge flows to estimate daily TP fluxes and the associated uncertainties. The daily estimates were then summed to generate annual fluxes.

We applied GAM to calculate the TP loads at the inflow and outflow locations of the St. Clair River and the inflow locations of the Detroit River and Niagara River. As both flow and TP concentrations in the downstream portion of the Detroit River are affected by water level fluctuations in the western basin of Lake Erie due to surface seiches, wind-driven water set-ups, and corresponding backflow, the annual TP load delivered by the Detroit River to the western basin of Lake Erie was estimated as the sum of the TP inflow flux from Lake St. Clair (21MICH-820,414; Table A7) plus the added TP loads from all the Detroit River's sub-watersheds. The TP outflow flux via the Niagara River was estimated with GAM using gauged flow data and river TP concentrations measured at ECCC's Fort Erie station (Fig. 1). Due to its proximity to the Niagara River, the Welland Canal's TP outflow flux was estimated by multiplying the reported daily canal water discharge by the same mean daily TP concentration as for the Niagara River.

The estimates of tributary point source loads reported here correspond to direct inputs downstream of the last monitoring station along a river course (Maccoux et al., 2016; Scavia et al., 2019a, 2019b); any upstream point source would have been captured by the monitoring data. The TP concentrations associated with direct groundwater inputs to Lake Erie were assumed equal to the median long-term TP concentrations observed in groundwater monitoring wells located within 8 km of the shoreline, which represents the zone where most lake water––ground water exchanges occur in the Laurentian Great Lakes (Xu et al., 2021). On the Canadian side of Lake Erie, TP concentration data are measured at 19 such groundwater monitoring wells covering all three basins (Table A9). Similar data, however, are not available for the United States side of Lake Erie (USGS, 2022). In addition, the Canadian groundwater TP concentrations are only analyzed once a year. Therefore, we decided to pool all of the available data from 2002 to 2019 to derive a single TP median concentration value that was then systematically applied over the entire study period.

Over-lake atmospheric wet TP deposition was calculated as the product of the volume-weighted mean rainwater TP concentration (p^{PR})

and the amount of precipitation. The p^{PR} values were based on data from three ECCC wet precipitation gauges located on the east shore of Lake St. Clair and, for Lake Erie, at Point Pelee and Rock Point (Fig. 1; Appendix A5). The stations' location coordinates and sampling methods are described in Chan et al. (2003), and the concentrations are reported by ECCC's Water Quality Monitoring and Surveillance Division (WQMSD, 2019). The over-lake precipitation rates used were those given in GLERL (2020b). Total (wet plus dry) over-lake TP deposition was estimated using the average wet and dry TP deposition ratio for the continental United States (Anderson and Downing, 2006).

Annual net TP sediment deposition rates for each of the three Lake Erie basins and Lake St. Clair were calculated using the post-1990 settling velocities of Chapra et al. (2016), the mean basin-specific TP concentrations and the corresponding lake bottom areas. The settling velocities reported by Chapra and coworkers in previous Lake Erie TP mass balance modeling are apparent parameters that were calibrated to reproduce observed average open lake concentrations (Chapra et al., 2016; Chapra and Dolan, 2012). As such, the effects of post-depositional processes at the lake floor, including recycling of P from the sediments back to the water column, are folded into the parameter values. In turn, this implies that using these apparent velocities should yield lower limits for our mass balance-derived internal P loads. As discussed further below, we speculate that our relatively large internal load estimates must in part reflect in-lake TP remobilization processes other than the classical, redox-dependent efflux of dissolved P from the lake floor, as already suggested by Chapra and Dolan (2012) and Chapra et al. (2016). It is useful to note that the apparent settling velocities used in estimating the internal TP loads in Lake Erie are in general agreement with the relatively sparse direct field-based measurements (Bloesch, 1982), as well as with the typical range of sedimentation rates of fine-grained sediments (Kemp et al., 1977; Mortimer, 1987) together with reported sediment TP concentrations in depositional areas of the Lake Erie basins (Williams et al., 1976; see Appendix A6 for further details).

The inter-basin TP exchanges in Lake Erie were calculated with the bulk horizontal eddy diffusion coefficients reported in Chapra et al. (2016) multiplied by the differences in the mean annual basin-specific TP concentrations between adjacent basins. Finally, the internal TP loads to the water column of Lake St. Clair and Lake Erie's basins that are mobilized by in-lake processes were determined as the differences between all the estimated external inputs and outputs averaged over the 14-year study period.

2.6. TP relative residence times

The TP relative residence time is a useful parameter to gauge the sensitivity of TP concentrations to in-lake processing (Janus and Vollenweider, 1984; Sonzogni et al., 1976). It equals the ratio of the mean TP residence time (R_p; yr) to the mean water residence time (R_w; yr). Using the water and TP budgets, we computed R_w and R_p for Lake Erie, its three basins, and Lake St. Clair: R_w was calculated as the ratio of the mean annual water volume (in km^3) to mean annual water supply (in $km^3 \, yr^{-1}$), while R_p was calculated as the mean annual standing stock of TP in the water column divided by annual external TP supply. For the St. Clair River and the Detroit River, literature values of R_w were used: 0.88 days for St. Clair River (Griffiths et al., 1991) and 0.83 days for Detroit River (Derecki, 1984).

3. Results

3.1. Watershed delineation

The entire Lake St. Clair–Lake Erie drainage basin (77,213 km^2) comprises two sub-basins: the 17,711 km^2 Huron Erie Corridor (HEC) watershed and Lake Erie's 59,501 km^2 direct watershed (Table 3; Fig. 2a). HEC includes the watersheds of Lake St. Clair (69% or 12,226 km^2), the Detroit River (11% or 1986 km^2), and the St. Clair River (20%

Table 3
Watershed areas (km^2) of the Lake St. Clair-Lake Erie system.

#	System	Total Area (TA)			Monitored Area (MA)			MA as % of TA [%]		
		Canada	USA	Total	Canada	USA	Total	Canada	USA	Total
1	HEC, including:	10,469	7242	17,711	6854	4936	11,790	65.5	68.2	66.6
1.1	St. Clair River	502	2997	3499	0	2031	2031	0.0	67.8	58.0
1.2	Lake St. Clair	9499	2727	12,226	6625	1901	8526	69.7	69.7	69.7
1.3	Detroit River	468	1518	1986	229	1005	1234	48.9	66.2	62.1
2	LE, including:	12,174	47,327	59,501	8724	36,594	45,318	70.4	77.3	75.9
2.1	West Basin	431	26,467	26,898	0	22,742	22,742	0.0	85.9	84.5
2.2	Central Basin	2710	14,764	17,474	1331	11,748	13,079	49.1	79.6	74.8
2.3	East Basin	9033	6096	15,129	7239	2104	9497	80.1	34.5	61.8
	Total (HEC + LE)	22,643	54,570	77,213	15,424	41,531	56,955	68.1	76.1	73.8

Abbreviations: Huron-Erie Corridor (HEC), Lake Erie (LE), watershed area (WA).

or 3499 km^2). The watersheds of Lake Erie's three basins include the western basin (45% or 26,898 km^2), central basin (29% or 17,474 km^2), and eastern basin (26% 15,129 km^2). The total area covered by hydrological and water quality data represents 74% of the total Lake Erie drainage basin (Table 3). While the Canadian portion of the HEC watershed is larger than the US portion (59% versus 41%), the US portion of the Lake Erie watershed is the largest at about 80% (Table 3; Fig. 2a).

3.2. Mean annual water budgets (2003 to 2016)

The volumes of Lake St. Clair and Lake Erie, averaged over the 14-year period, were 4.6 and 501.0 km^3 (Table 4). Lake Erie''s total volume was divided into the western (5.4% or 27.2 km^3), central (63.0% or 315.5 km^3), and eastern (31.6% or 158.1 km^3) basins. The mean volumes of the St. Clair River and Detroit River channels were about 0.4 km^3 each (Table 4). The surface area of Lake St. Clair was estimated at 1114 km^2, that of Lake Erie's at 25,657 km^2 (Table 4). Lake Erie's basin surface areas were 3284 km^2, 16,138 km^2, and 6235 km^2 for the western, central, and eastern basins, respectively.

Although there are many tributaries to the Lake St. Clair–Lake Erie system (Fig. 1; Table 5) their flow contributions are relatively small compared to the flow rates of the connecting channels. The St. Clair River flow averaged 5042 and 5068 $m^3\ s^{-1}$ at the channel's inlet and mouth (Tables 6, 7, B1 to B4; Fig. 2b), respectively. Lake St. Clair added only 2.8% to the inflow from the St. Clair River, yielding an outflow to the Detroit River of 5212 $m^3\ s^{-1}$. The Detroit River flow increased by 23 $m^3\ s^{-1}$ to 5235 $m^3\ s^{-1}$ at the outflow into the western basin of Lake Erie. Lake Erie's direct watersheds added 13.4% to the Detroit River flow for a total Lake Erie outflow of 5935 $m^3\ s^{-1}$ divided between the Niagara River (96.7% or 5740.2 $m^3\ s^{-1}$) and the Welland Canal (3.3% or 194.5 $m^3\ s^{-1}$). Watershed inflows to Lake St. Clair and Lake Erie were estimated at 142 and 799 $m^3\ s^{-1}$, respectively.

On average, over-lake evaporation (31 and 716 $m^3\ s^{-1}$) exceeded precipitation (27 and 651 $m^3\ s^{-1}$) by about 15% and 10% in Lake St. Clair and Lake Erie, respectively (Tables 6, 7, B1 to B4; Fig. 2b-c). Consumptive water usage was very small (<0.5% of total lake inflow) with a mean value of 23.5 $m^3\ s^{-1}$. The net losses in lake storage were minor for both Lake St. Clair and Lake Erie (1.4 and 21.5 $m^3\ s^{-1}$, respectively), or <0.03% and 0.4% of the lakes' outflows. Diversions from Lake Huron by the Detroit Water Treatment Plant (Huron WTP) and groundwater recharge were the smallest fluxes, accounting for 7 $m^3\ s^{-1}$ and 12 $m^3\ s^{-1}$, respectively.

3.3. Mean annual TP mass budget (2003 to 2016)

Lake Erie's TP standing stock (5012 MT, Table 4) was equivalent to 45% of the lake's yearly external input of TP (11,116 MTA; see Figs. 3 & 4; Table 8). The TP standing stocks of the western, central, and eastern basins were 540 MT, 3311 MT, and 1161 MT, respectively. Lake St. Clair had a standing stock of 69 MT, and the St. Clair River and Detroit River

channels had standing stocks of 5 and 7 MT, respectively (Table 4).

The mean atmospheric deposition of TP (Table A10) ranged from 52 MTA for Lake St. Clair to 992 MTA for Lake Erie, with 127 MTA, 624 MTA and 241 MTA for the western, central, and eastern basins, respectively (Fig. 3a-b; Tables 8, B7, B9 to B11). The over-lake atmospheric TP loading represented <10% of the total external load for the entire Lake St. Clair–Lake Erie system (1044 versus 11,703 MTA; Table 8). Fluxes associated with changes in lake volume, consumptive use, and ground water were all less important (Fig. 3). The median groundwater TP concentration was about 20 mg P m^{-3} (Table 9).

The largest external TP input to the Lake St. Clair–Lake Erie system (8797 MTA) originated from the direct watersheds, with 3020 MTA, 2538 MTA, and 1455 MTA inputs to the western, central, and eastern basins, respectively, 911 MTA to Lake St. Clair; and 208 MTA and 665 MTA to the St. Clair River and Detroit River, respectively (Table 8). The mean input flux of TP from Lake Huron to the St. Clair River was 1862 MTA (Fig. 3a; Tables 6, 8, B6) and included 1100 MTA derived using the monitoring data for the inflow from Lake Huron to the St. Clair River plus an estimated 762 MTA generated by episodic events of coastal erosion and resuspension that are not captured by the monitoring data (Scavia et al., 2019a, 2019b, 2020, 2022). Including contributions from the St. Clair River watershed (208 MTA), the total load delivered by the St. Clair River to Lake St. Clair was then 2070 MTA.

The largest tributary to Lake St. Clair in terms of TP load was the Thames River with a mean annual load of 429 MTA followed by the Sydenham and Clinton rivers (170 and 145 MTA, respectively; Fig. 1; Table 5). For Lake Erie, the Maumee River was by far the most significant source of TP to the lake delivering alone a mean annual load of 2428 MTA, followed by the Sandusky (701 MTA) and Grand Ontario (346 MTA) rivers.

The TP outflow from Lake Erie via the Niagara River was estimated at 4834 MTA using a mean TP concentration of 27 μg P L^{-1} based on measurements of the inflow to the Niagara River (Fig. 3; Table 6, B4 & B11). The annual loss of TP via the Niagara River plus the Welland Canal then amounted to 4997 MTA. Our Niagara River outflow flux of 4834 MTA is close to the mean value of 4791 MTA obtained by Hill and Dove (2021) who used data for the 2014–2018 period. Note that the TP concentrations measured in the waters of the Niagara River are significantly higher than the offshore TP concentrations of the eastern basin of Lake Erie (mean = 7.3 μg P L^{-1}; Table B5; Appendix A7).

The removal of TP from Lake Erie's water column through sedimentation at the lake floor was comparable in magnitude to the watershed TP loading (Fig. 3; Tables 8, B6, B9 to B11): 807 MTA for Lake St. Clair and 9676 MTA for Lake Erie divided into 3188 MTA, 5032 MTA, and 1455 MTA for the western, central, and eastern basin, respectively. Expressed per unit surface area, the TP deposition fluxes were 0.97, 0.31, and 0.23 g P $m^{-2}\ yr^{-1}$ in the western, central, and eastern basin, respectively, while in Lake St. Clair the rate was 0.72 g P $m^{-2}\ yr^{-1}$ (Table 8). TP fluxes associated with changes in net water storage were small and insignificant relative to other inputs and output pathways (Tables 6, 8, B6 to B11; Fig. 3).
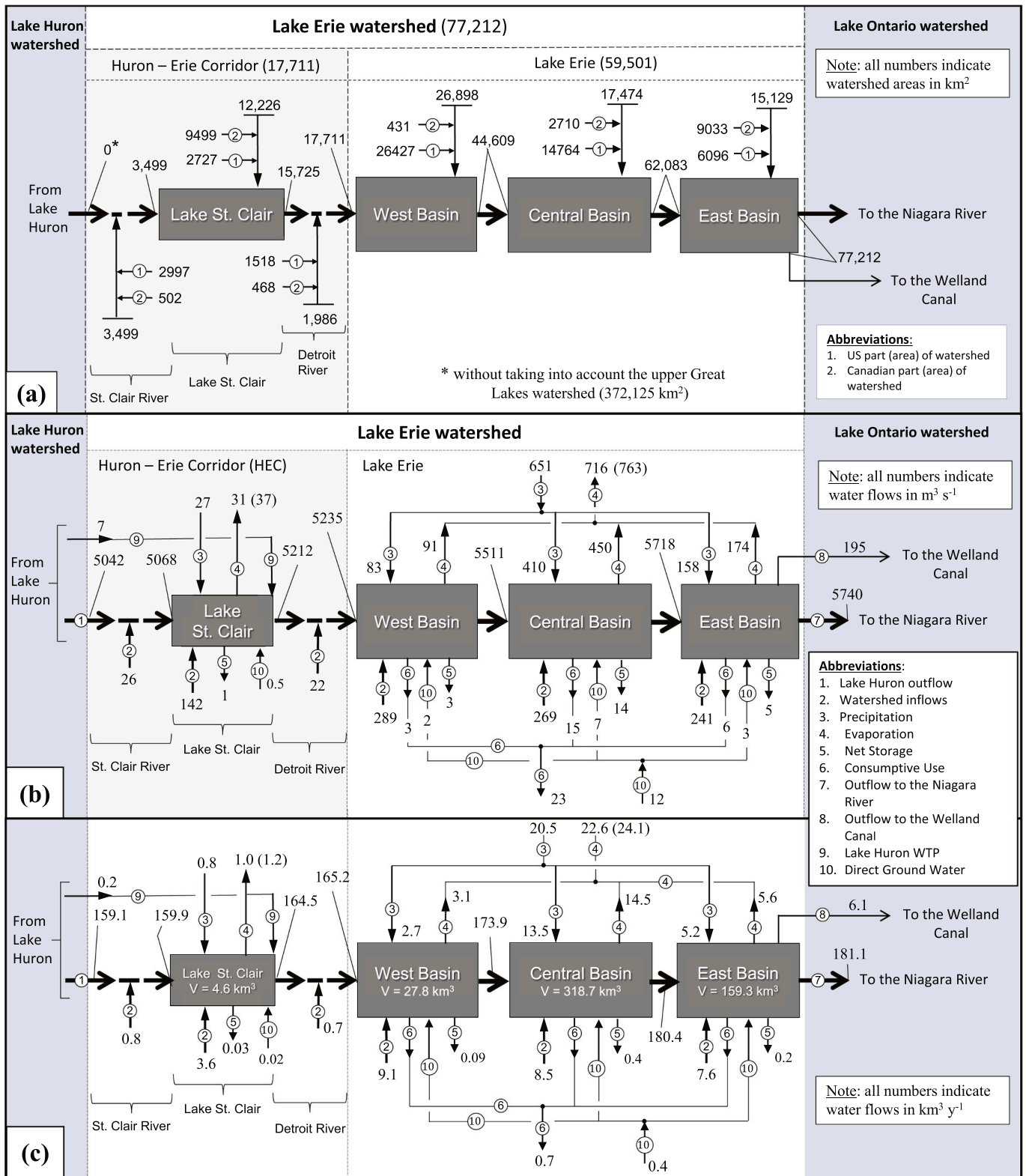
Fig. 2. (a) Surface areas of the sub-watersheds of the Lake St. Clair–Lake Erie system, including total area and respective areas in the United States and Canada. (b, c) Mean water budget of Lake St. Clair–Lake Erie system averaged over the 2003 to 2016 period, with (b) water fluxes in $m^3 \, s^{-1}$ and (c) in $km^3 \, yr^{-1}$. For the evaporative fluxes in b and c, the numbers in brackets are the original values which were adjusted to close the water budget. Numbers shown inside the boxes indicate the average annual water volumes in km^3.

Table 4
Mean water volumes* (V), surface areas (A), mean depths (Z_m), water residence times (R_w), total phosphorus (TP) residence times (R_p), ratios of R_p to R_w, and standing stocks of TP in water column. All values are averages for the 2003–2016 period.

Segment	V	A	Z_m	R_w	R_p	R_p/R_w	TP standing stock in water column [metric tons]		
	[km³]	[km²]	[m]	[day]	[day]	[–]	April	August	Average
St. Clair River	~0.4	–	–	0.88[#]	0.88	1.00	–	–	~5
Lake St. Clair	4.6	1114	4.1	10	8	0.81	–	–	69
Detroit River	~0.4	–	–	0.83ˆ	0.83	1.00	–	–	~7
Lake Erie, including:	505.8	25,657	19.7	953	312	0.33	6328	3699	5012
- Western Basin	27.8	3284	8.5	57	31	0.55	643	437	540
- Central Basin	318.7	16,138	19.7	595	180	0.30	4153	2473	3311
- Eastern Basin	159.3	6235	25.5	301	101	0.34	1532	789	1161

Note: * Based on mean water levels over 2003 to 2016 period: 175.95 (Lake St. Clair) and 174.16 (Lake Erie) meters above International Great Lakes Datum (1985); [#], Griffiths et al. (1991); ˆ, Derecki (1984); Z_m, mean depth, calculated as the mean volume (V) divided by the mean area (A); summed numbers may not add up exactly due to rounding effects.

Table 5
Selected major tributaries, rivers (R.) and creeks (Cr.) discharging into the Lake St. Clair–Lake Erie system: names, drainage areas, mean annual flows and mean total phosphorus loads for the period 2003 to 2016. For the locations of the tributaries see Fig. 1.

ID #	Tributary Name, State/Province	Receiving segment	Drainage area (km²)	Mean annual flow (m³ s⁻¹)	Mean annual TP load (MTA)
1.	Black R., MI	St. Clair	1841	13.2	95
2.	Belle R., MI	River	589	4.7	35
3.	Pine R., MI		487	3.9	28
4.	Clinton R., MI	Lake St.	1916	19.5	145
5.	Sydenham R., ON	Clair	2676	28.7	170
6.	Thames R., ON		5875	74.3	429
7.	Rouge R., MI	Detroit	1230	13.8	107
8.	Canard T., ON	River	347	4.0	17
9.	Huron R., MI	Western	2378	19.3	29
10.	Raisin R., MI	Basin	2753	24.3	133
11.	Ottawa R., OH		448	4.3	22
12.	Maumee R., OH, MI, IN		17,019	190.8	2428
13.	Cedar Cr., OH		537	6.9	71
14.	Toussaint R., OH		370	4.8	49
15.	Portage R., OH		1614	20.8	214
16.	Sandusky R., OH	Central	3970	52.3	701
17.	Huron R., OH	Basin	1051	14.1	139
18.	Vermilion R., OH		694	9.3	92
19.	Black R., OH		1458	21.5	191
20.	Rocky R., OH		686	10.1	90
21.	Cuyahoga R., OH		2102	41.7	322
22.	Chagrin R.,		686	14.0	67
23.	Grand R., OH		1828	32.8	243
24.	Ashtabula R., OH, PA		329	6.7	32
25.	Conneaut Cr., OH, PA		163	3.4	16
26.	Big Otter Cr., ON		729	9.8	87
27.	Catfish Cr., ON		393	4.7	43
28.	Kettle Cr., ON		478	5.6	49
29.	Chautauqua Cr., NY	Eastern	207	4.3	20
30.	Cattaraugus Cr., NY	Basin	1450	29.2	304
31.	Eighteenmile Cr., NY		311	5.9	61
32.	Buffalo R., NY		1049	20.0	205
33.	Grand R., ON		6775	84.2	346
34.	Nanticoke Cr., ON		199	2.2	11
35.	Lynn R., ON		172	2.2	5
36.	Big Cr., ON		741	9.7	26

The combined output estimates systematically exceeded the external inputs, especially for Lake Erie. To balance the TP budgets, 3563 and 220 MTA had to be added to the water columns of Lake Erie and Lake St. Clair, respectively. For Lake Erie's basins, the extra, in-lake sourced TP amounted to 495 MTA for the western basin, 795 MTA for the central basin, and 2273 MTA for the eastern basin (Fig. 3b; Table 8).

3.4. TP relative residence times

The mean hydraulic residence times (R_w) ranged from 10 days for Lake St. Clair to 953 days (~2.6 years) for Lake Erie (Table 4), with 57 days for the western, 595 days for the central, and 301 days for the eastern basin. Mean TP residence times (R_p) were systematically shorter than hydraulic residence times (Table 4): R_p was 8 days in Lake St. Clair and 312 days in Lake Erie, with 31, 180, and 101 days for the western, central, and eastern basins, respectively. The TP relative residence times (R_p:R_w ratios, Table 4) were 0.81 for Lake St. Clair, with values of 0.55 for the western basin, 0.30 for the central basin, and 0.34 for the eastern basin of Lake Erie. The R_p:R_w values for the St. Clair River and Detroit River channels were indistinguishable from 1.

4. Discussion

Earlier Lake Erie phosphorus mass balances, generally based on data for one or only a few years (Burns, 1976; Chapra, 1977; Chapra et al., 2016; Chapra and Dolan, 2012; Chapra and Sonzogni, 1979), have yielded valuable information on historical external loads and their role in eutrophication. The 14-year averaged, post-2000 TP mass balance for Lake Erie presented here extends these previous studies by capturing the long-term TP cycling, that is, at time scales significantly exceeding the hydraulic residence time of the overall lake system (Appendix A1). At such time scales, the assumptions of steady state water and TP budgets provide useful approximations to compare the magnitudes of TP inputs and outputs for the entire lake system as well as those for individual basins (Appendix A7). As we show, this comparison leads to the unavoidable conclusion that a significant fraction of the TP entering the water column comes from sources that are activated by in-lake processes. In the following sections, the TP budgets of Lake St. Clair and Lake Erie's three basins are discussed.

4.1. Lake St. Clair

Our estimate of the mean annual TP load to Lake St. Clair originating from Lake Huron (1862 MTA) is up to three times higher than some earlier proposed values (e.g., Dolan, 1993; Dolan and Chapra, 2012; Dolan and McGunagle, 2005; Maccoux et al., 2016), but in agreement with more recent assessments (Burniston et al., 2018; Scavia et al., 2019a, 2019b, 2020, 2022). According to our results, Lake Huron contributes 90% of the TP load carried by the St. Clair River, with the remaining 10% coming from St. Clair River's direct watershed. It further

Table 6

Mean annual water and phosphorus budgets for the Lake St. Clair–Lake Erie system for the 2003 to 2016 period.

|	Component	Water Budget (m^3 s^{-1})			Phosphorus Budget (MTA)		
		USA	Canada	Total	USA	Canada	Total
A. Lake Erie Indirect Watersheds:							
1. St. Clair River watershed:							
1.1	Inflow (at the inlet), including:			5042.0			1862.3
	- load captured by monitoring programs						1100.3
	- load missed by monitoring programs						762.0
1.2	watershed loads	22.0	4.1	26.1	163.4	44.5	207.9
1.3	at the mouth			5068.1			2070.2
2. Lake St. Clair watershed:							
2.1	inflow (St. Clair River)			5068.1			2070.2
2.2	watershed inflow/input	28.3	113.7	142.0	211.0	700.4	911.3
2.3	Precipitation/Atmospheric deposition			26.7			52.1
2.4	Evaporation (Overlake)			−30.6			–
2.5	Net storage change			−1.4			−0.5
2.6	Consumptive use			0.0			0.0
2.7	Huron WWT			7.0			0.0
2.8	Direct ground water discharge			0.5			0.3
2.9	Sedimentation						−806.9
2.10	Internal Load						220.3
2.11	Outflow			5212			2446.9
3. Detroit River watershed:							
3.1	at the source (Lake St. Clair outflow)			5212.3			2446.9
3.2	watershed inflow/input	17.0	5.4	22.4	624.6	40.9	665.5
3.3	outflow (Detroit River at the mouth)			5234.7			3112.4
B. Lake Erie Direct Watersheds:							
4. Lake Erie (all three basins):							
4.1	inflow (Detroit River)			5234.7			3112.4
4.2	Western basin inflow/input	284.1	5.3	289.4	2996.7	23.0	3019.7
4.3	Central basin inflow/input	235.2	33.3	268.5	2278.4	259.8	2538.2
4.4	Eastern basin inflow/input	122.0	118.8	240.8	993.7	460.9	1454.7
4.5	Precipitation/Atmospheric deposition			650.7			992.1
4.6	Evaporation (Overlake)			−716.1			–
4.7	Net Storage			−21.5			−6.2
4.8	Consumptive Use			−23.5			−8.0
4.9	Direct ground Water discharge			11.5			7.3
4.10	Sedimentation						−9675.7
4.11	Internal Load, including:						3562.6
	- Western Basin						495.4
	- Central Basin						794.5
	- Eastern Basin						2272.6
4.12	Estimated Output (TOTAL), including:			5934.7			
	- Niagara River			5740.2			−4833.9
	- Welland Canal			194.5			−163.2

Table 7

Segment-specific total (m^3 s^{-1}) and areal (m yr^{-1}) rates of water inputs and losses: watershed inputs (*W*), over-lake precipitation (*P*) and evaporation (*E*), inter-segment exchanges (*IB*), consumptive water use (*CU*), direct ground water discharge (*GR*), and water storage change (*ΔV*) for St. Clair River (SCR), Lake St. Clair (LSC), Detroit River (DR), Western Basin (WB), Central Basin (CB), Eastern Basin (EB), Lake Erie (LE), and Lake St. Clair–Lake Erie System (LES).

#	Rates (units)	Loads / Losses	SCR	LSC	DR	WB	CB	EB	LE	LES
1.		*W*	26.1	142.0	22.4	289.3	268.6	240.8	798.7	989.2
		P	–	26.7	–	83.3	409.3	158.1	650.7	677.4
		E	–	−30.6	–	−91.7	−450.4	−174	−716.1	−746.7
		IB	5042.0	5068.1	5212.3	5234.7	5511.5	5717.9	5234.7	5042.0
	Total rates (m^3 s^{-1})	Huron WTPˆ	–	7.0	–	–	–	–	–	7.0
		CU	–	–	–	−3.0	−14.8	−5.7	−23.5	−23.5
		GR	–	0.5	–	1.5	7.2	2.8	11.5	12.0
		ΔV	–	−1.4	–	−2.8	−13.5	−5.2	−21.5	−22.9
		Segment outflow	5068.1	5212.3	5234.7	5511.5	5717.9	5934.7	5934.7	5934.7
2.		*W*	–	4.0	–	2.8	0.5	1.2	1.0	–
	Areal rates* (m yr^{-1})	*P*	–	0.8	–	0.8	0.8	0.8	0.8	–
		E	–	−0.9	–	−0.9	−0.9	−0.9	−0.9	–
		IB	–	143.6	–	50.3	10.8	28.9	6.5	–

Note: * Total rates normalized to the segment surface area; ˆHuron WTP, Huron Water Treatment Plant.

implies that TP sourced from Lake Huron represents the largest fraction (61%) of the total external TP input to Lake St. Clair, with the latter estimated at 3042 MTA. In comparison, 2447 MTA leave Lake St. Clair and flow into the Detroit River. Thus, about 19% of the external TP load to Lake St. Clair is retained in the lake (Table 6), which agrees with previous estimates (17%, Bocaniov et al., 2019; 21%, Scavia et al., 2019b), hence illustrating the important role Lake St. Clair plays in moderating the TP input into the western basin of Lake Erie.
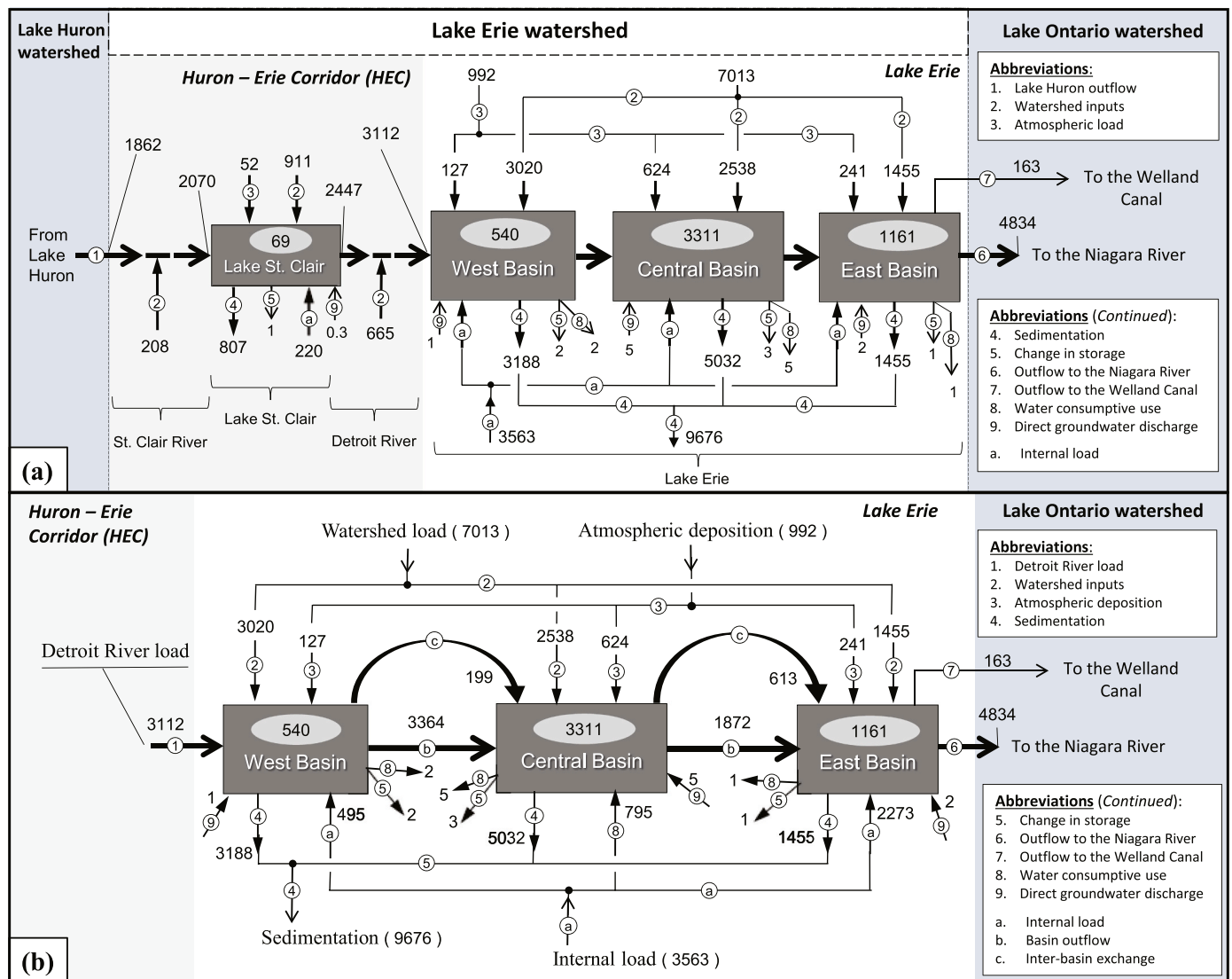
Fig. 3. (a) Mean TP fluxes (2003 to 2016) in metric tonnes per annum (MTA) for the major segments of the Lake St. Clair–Lake Erie system, with (b) showing additional details for the three basins of Lake Erie. Numbers shown inside the boxes indicate the average annual standing stocks of TP in MTA. Summed loadings may not add up exactly due to rounding errors.

Lake St. Clair's mean internal TP load is estimated at 220 MTA (Fig. 3a; Table 8). While this is about one order of magnitude less than the external TP load, it is still a significant input considering the water column TP standing stock of 69 MT (Table 4). A priori, a large internal TP load may not be expected given that Lake St. Clair is shallow and well mixed. Thus, a high internal P loading from the lake floor driven by bottom water hypoxia (e.g., Parsons et al., 2017) would seem unlikely. Other mechanisms, however, might be involved. For instance, the Thames River discharge is extremely low in summer (Bocaniov et al., 2019) and the downstream river reach itself may stratify vertically for a few days to a week or longer. The river is located in a fertile fluvial valley and carries high loads of fine-grained sediments enriched with nutrients (Stone and Saunderson, 1992, 1996). Nürnberg and LaZerte (2015) have suggested that this material can create a high sediment oxygen demand and generate hypoxic episodes that may release highly bioavailable P from the river sediments, which is then transported to the lake. Furthermore, mixing of bottom sediments by shear stress can release pore water and contribute to internal P loading as well (Tammeorg et al., 2022).

Another potential TP source is loading from the St. Clair River delta.

The lower reach of the St. Clair River empties into the lake through a unique "burrowing" delta that slowly propagates downstream causing erosion and lakeward transport of older sediment (Thomas et al., 2006). The eroded material with the associated P enters the lake but is not captured by the water quality monitoring stations in the St. Clair River because these stations are located upstream of the delta (see Fig. 1, water quality monitoring stations #3 and #4). Our mass balance results therefore reinforce the need to consider internal P loading mechanisms other than the "classical" redox-sensitive benthic P recycling from recently deposited sediments.

4.2. Western Basin

The external TP load entering Lake Erie's western basin via the Detroit River (3112 MTA; Tables 6 & 8; Fig. 3) is of similar magnitude as the combined external load supplied from the western basin's direct watershed plus atmospheric deposition and direct groundwater input (3148 MTA). The net internal TP load of the western basin is estimated at 495 MTA (Tables A1 & 8; Fig. 3b). In the western basin, a major internal P loading pathway is likely dissolved P efflux from the lake
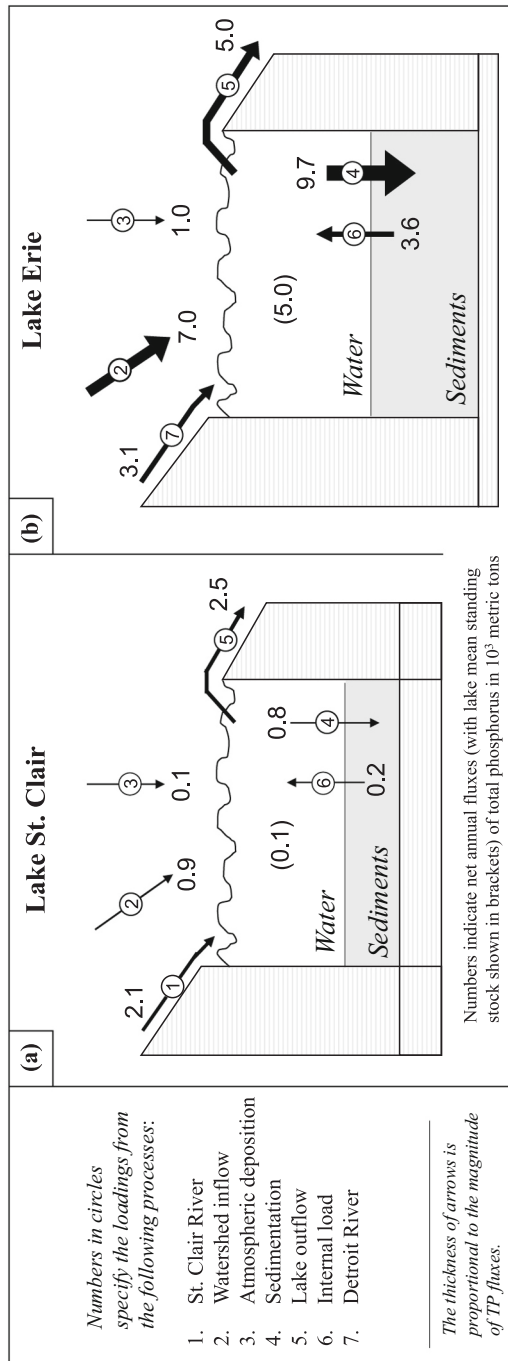
Fig. 4. Simplified conceptual diagram of mean total phosphorus (TP) inputs and outputs (in 1000s of MTA) for Lake St. Clair (a) and Lake Erie (b) for the period of 2003 to 2016 based on the results presented in Fig. 3.

bottom sediments under reducing conditions (Gibbons and Bridgeman, 2020; Matisoff et al., 2016; Parsons et al., 2017) during intermittent bottom water hypoxia (Jabbari et al., 2019, 2021; Rowe et al., 2019). Nonetheless, other processes may also be involved, for example, the supply of sediment-bound P via the Detroit River (Colborne et al., 2019).

Matisoff et al. (2016) estimated the gross internal P load to the western basin in 2013 and 2014 to be around 593 MTA (range: 378 to 808 MTA; Table A1, ID#1), close to our 495 MTA estimate (Fig. 3b). Phosphorus released from the bottom sediments is expected to be rapidly incorporated into the food web, because intermittent hypoxia that usually occurs from June to September (Jabbari et al., 2019) overlaps with the formation of cyanobacterial blooms in June to early October (Sayers et al., 2019). Thus, in addition to the Maumee River's spring TP loads that drive most cyanobacterial bloom models (Bertani et al., 2016; Scavia et al., 2021; Stumpf et al., 2016), the hypoxia-induced internal TP load could provide an additional bioavailable P supply sustaining algal growth during summer-early fall, as proposed by Matisoff et al. (2016). This explanation is also consistent with Ho and Michalak (2017) and Scavia et al. (2023) who reported improved model performance when the cumulative P load from previous years was added as a surrogate for the P internal load.

Sediments in the western basin have been shown to be a source of biologically available P and chemically reduced forms of N (e.g., NH_4^+) that can contribute to support the non-nitrogen-fixing cyanobacterial HABs (Microcystis blooms) typical of the western basin (Boedecker et al., 2020). The estimated magnitude of the internal TP loading in the western basin, however, is small compared to the basin's external load (495 versus 6256 MTA; Table 8). Thus, while the external TP load is undeniably the main driver of HABs in the western basin, internal loading from bottom sediments could be an additional, subtler, factor modulating HAB dynamics in the basin – a role that deserves to be investigated further.

4.3. Central Basin

Similar to the western basin, the TP loading to Lake Erie's central basin from the upstream lake segment (3563 MTA) is of comparable magnitude to that supplied from the direct watershed plus atmospheric deposition and direct groundwater input (3167 MTA). The Central Basin also exhibits one of the largest known freshwater hypoxic zones in the world with a maximum extent of up to 12,000 km^2 (Zhou et al., 2013; Bocaniov and Scavia, 2016; Bocaniov et al., 2016, 2020). Hence, among Lake Erie's three basins, the central basin might be expected to be most impacted by internal TP loading from sediments overlain by anoxic bottom waters.

Based on our mass balance calculations, net internal TP loading contributes 795 MTA, which fall in the range of 300 to 2400 MTA proposed by Paytan et al. (2017) (see Nürnberg et al., 2019, for a critical analysis of this range). Some recent studies have reported much larger benthic P effluxes for the central basin, between 10,000 and 11,000 MTA (Anderson et al., 2021; Wang et al., 2021). The reason for the large differences between the latter estimates and ours is not certain but may reflect a less efficient incorporation of P released from the bottom sediments into the food-web compared to the western basin. In turn, this could reflect the restricted upward transfer of the released P to the photic zone during summer when the water column is stratified. In addition, following fall turnover and the return of oxygenated conditions, dissolved phosphate may be scavenged by oxidized Fe phases settling to the lake floor (Burns and Nriagu, 1976; Manning et al., 1984). Not unexpectedly, this suggests significant differences in the fate of the internal P load released during the short-lived intermittent hypoxic events in the shallow western basin and that produced by the longer-duration stratification and hypolimnetic hypoxia of the deeper central basin.

Table 8

Segment-specific total (MTA) and areal (g P m^{-2} yr^{-1}) rates of total phosphorus (TP) inputs and losses: watershed inputs (*W*); inputs and losses due direct ground water discharge, water consumptive use, and change in water storage (*GR*, *CU* and ΔV, respectively); over-lake total atmospheric deposition (*A*); inter-segment exchanges (*IB*); internal loads (*L*), and sedimentation losses (*S*). See Table 7 for the segment full names.

#	Rates (units)	Loads / Losses	SCR	LSC	DR	WB	CB	EB	LE	LES
1.		*W*	208	911	665	3020	2538	1455	7013	8797
		GR	–	0.3	–	0.9	4.5	1.8	7.3	7.6
		CU	–	–	–	−1.9	−4.8	−1.3	−8.0	−8.0
		ΔV	–	−0.5	–	−2.2	−2.8	−1.1	−6.2	−6.7
		$W^{\#} = W + GR + CU$	208	912	665	3019	2538	1455	7012	8797
		$W^{\#\#} = W + GR + CU + \Delta V$	208	911	665	3017	2535	1454	7006	8790
		A	–	52	–	127	624	241	992	1044
		IB	1862	2070	2447	3112	3563	2485	3112	1862
	Total rates (MTA)	*L*	–	220	–	495	795	2273	3563	3783
		$W + A + GR$	208	964	665	3148	3167	1697	8012	9849
		$W^{\#} + A$	208	963	665	3146	3162	1696	8004	9841
		$W^{\#} + A + IB$	2070	3034	3112	6258	6725	4181	11,116	11,703
		$W^{\#} + A + IB + L$	2070	3254	3112	6754	7520	6453	14,679	15,486
		$W^{\#\#} + A$	208	963	665	3144	3159	1695	7998	9835
		$W^{\#\#} + A + IB$	2070	3033	3112	6256	6722	4180	11,110	11,697
		$W^{\#\#} + A + IB + L$	2070	3254	3112	6752	7517	6452	14,673	15,479
		S		807		3188	5032	1455	9676	10,483
		Segment outflow	2070	2447	3112	3563	2485	4997	4997	4997
2.		$W^{\#\#}$	–	0.818	–	0.919	0.157	0.233	0.273	0.328
		A	–	0.047	–	0.039	0.039	0.039	0.039	0.039
		IB	–	1.858	–	0.948	0.221	0.399	0.121	0.070
	Areal rates* (g P m^{-2} yr^{-1})	*L*	–	0.198	–	0.151	0.049	0.364	0.139	0.141
		$W^{\#\#} + A$	–	0.865	–	0.957	0.196	0.272	0.312	0.367
		$W^{\#\#} + A + IB$	–	2.723	–	1.905	0.417	0.670	0.433	0.437
		$W^{\#\#} + A + IB + L$	–	2.921	–	2.056	0.466	1.035	0.572	0.578
		S	–	0.724	–	0.971	0.312	0.233	0.377	0.392

Note: * Basin-wide rates normalized to the segment surface area.

Table 9

Total phosphorus (TP) concentrations (mg P L^{-1}) in ground water monitoring wells within 8 km of lake shorelines for the period of 2002 to 2019.

Location	# of wells	*N*	*Mean*	*SD*	*Median*
Lake Erie Basin, including:	19	179	0.068	0.137	0.020
- Western Basin	6	68	0.026	0.069	0.012
- Central Basin	8	69	0.115	0.173	0.032
- Eastern Basin	5	42	0.060	0.133	0.020

Note: *N*, number of observations; *Mean*, mean value, *SD*, standard deviation; *Median*, median value; for groundwater well locations and well characteristics see Table A9.

4.4. Eastern Basin

The eastern basin is the coldest and deepest of Lake Erie's three basins. The largest fraction of the external TP loading to the eastern basin is supplied from the upstream central basin (59%, 2485 MTA) with a somewhat smaller contribution from the watershed, atmospheric deposition plus groundwater inputs (41%, 1699 MTA). In contrast to the other two basins, the eastern basin does not experience substantial bottom water hypoxia, nor is it affected by large cyanobacterial blooms. The estimated internal TP load for the eastern basin (2273 MTA; Fig. 3b), however is the largest of the three basins. In contrast to the two other basins of Lake Erie, the net internal TP load of the eastern basin exceeds the basin's combined external input from its watershed and airshed.

The "classical" internal P loading mechanism where dissolved P is released from recently deposited sediments in response to bottom water hypoxia cannot explain the inferred large internal TP load. Not only are hypoxic bottom water conditions relatively rare but the estimated P settling rate in the eastern basin is also the lowest of the three basins (0.23 g P m^{-2} yr^{-1}, Section 3.3). Thus, other in-lake processes must be responsible for generating the internal TP loading of the eastern basin. These may include shoreline erosion and resuspension, not unlike the delivery of Lake Huron sediment-bound TP to Lake St. Clair (see Section 4.1), as well as the nearshore phosphorus shunt caused by the filtering activity of invasive dreissenid mussels (Bocaniov et al., 2014; Hecky et al., 2004). Chapra and Dolan (2012) further suggested that apart from shoreline erosion and mussel grazing other input pathways may be involved, for example nearshore P assimilation during benthic macro-algal blooms (e.g. *Cladophora*) and the subsequent nearshore transport of biomass-associated P to the eastern basin's outlet after bloom collapse. These processes would result in the preferential P enrichment of the coastal waters of the basin, which subsequently flow out of Lake Erie via the Niagara River and Welland Canal. While speculative, this explanation would also account for the relatively high TP concentrations measured at the mouth of the Niagara River (27 μg P L^{-1}, Section 3.3).

4.5. Relative TP residence times

The relative TP residence times (R_p/R_w) provide a measure of the role in-lake processes play in controlling the TP standing stock of a water body. If TP behaves as a conservative tracer, then R_p/R_w is equal to 1 (Janus and Vollenweider, 1984). This is the case for both the St. Clair River and the Detroit River (Table 4). All P entering these channels is rapidly ($<$ 1 day) transferred to the downstream lake segment with negligible in-channel processing. In the lake basins, however, R_p/R_w values deviate from 1. The R_p/R_w value for Lake St. Clair ($R_p/R_w = 0.81$) is still relatively close to 1, in line with the relatively short water residence time and, hence, limited time for extensive P cycling in the lake basin. The much lower overall value for Lake Erie ($R_p/R_w = 0.33$) reflects the much longer water residence time (2.6 years; Table 4) that enables a large in-lake retention of P. Of the 11,116 MTA combined external loading to the three basins of Lake Erie, only 4997 MTA exit the lake via the Niagara River and Welland Canal. Burial of P in sediments accounts for almost all the missing 6119 MTA, with only 0.2% attributed to the change in water column storage and consumptive use.

4.6. Some implications

The important role internal nutrient loads play in modulating the trophic state of lake ecosystems is well recognized (Boström et al., 1982;

Ekholm et al., 1997; Ho and Michalak, 2017; Isles et al., 2015; Markelov et al., 2019; O'Connell et al., 2020; Orihel et al., 2017; Soranno et al., 1997; Yang et al., 2020). The budget estimations presented here imply that this is also the case for the large Lake St. Clair–Lake Erie system. Our estimates suggest that internal P supply to the water column represents close to a quarter of the total (external plus internal) P input to the entire system. It explains why models of algal blooms in the western basin that include a surrogate for the internal P load (Ho and Michalak, 2017; Scavia et al., 2023) may perform better compared to existing statistical (e.g. Bertani et al., 2016; Stumpf et al., 2016) and mechanistic ecological models that do not account for internal P loading.

Declaration of Competing Interest

Data availability

Datasets used within this study can be obtained from public sources described in Data and Methods section of this paper. Additionally, data are also openly available from the Federated Research Data Repository (FRDR) website at DOI:10.20383/102.0695

Acknowledgements

Appendix. Supplementary Data A and B

Supplementary data to this article can be found online at https://doi.org/10.1016/j.ecoinf.2023.102131.

References

Anderson, K.A., Downing, J.A., 2006. Dry and wet atmospheric deposition of nitrogen, phosphorus and silicon in an agricultural region. Water Air Soil Pollut. 176, 351–374.

Anderson, H.S., Johengen, T.H., Godwin, C.M., Purcell, H., Alsip, P.J., Ruberg, S.A., Mason, L.A., 2021. Continuous in situ nutrient analyzers pinpoint the onset and rate of internal P loading under anoxia in Lake Erie's Central Basin. ACS ES&T Water 1, 774–781.

Bertani, I., Obenour, D.R., Steger, C.E., Stow, C.A., Gronewold, A.D., Scavia, D., 2016. Probabilistically assessing the role of nutrient loading in harmful algal bloom formation in western Lake Erie. J. Great Lakes Res. 42, 1184–1192.

Bloesch, J., 1982. Inshore–offshore sedimentation differences resulting from resuspension in the eastern basin of Lake Erie. Can. J. Fish. Aquat. Sci. 39, 748–759.

Bocaniov, S.A., Scavia, D., 2016. Temporal and spatial dynamics of large lake hypoxia: integrating statistical and three-dimensional dynamic models to enhance lake management criteria. Water Resour. Res. 52, 4247–4263.

Bocaniov, S.A., Scavia, D., 2018. Nutrient loss rates in relation to transport time scales in a large shallow lake (Lake St. Clair, USA – Canada): insights from a three-dimensional lake model. Water Resour. Res. 54, 3825–3840.

Bocaniov, S.A., Smith, R.E., Spillman, C.M., Hipsey, M.R., Leon, L.F., 2014. The nearshore shunt and the decline of the phytoplankton spring bloom in the Laurentian Great Lakes: insights from a three-dimensional lake model. Hydrobiologia 731, 151–172.

Bocaniov, S.A., Leon, L.F., Rao, Y.R., Schwab, D.J., Scavia, D., 2016. Simulating the effect of nutrient reduction on hypoxia in a large lake (Lake Erie, USA-Canada) with a three-dimensional lake model. J. Great Lakes Res. 42, 1228–1240.

Bocaniov, S.A., Van Cappellen, P., Scavia, D., 2019. On the role of a large shallow lake (Lake St. Clair, USA-Canada) in modulating phosphorus loads to Lake Erie. Water Resour. Res. 55, 10548–10564.

Bocaniov, S.A., Lamb, K.G., Liu, W., Rao, Y.R., Smith, R.E., 2020. High sensitivity of lake hypoxia to air temperatures, winds and nutrient loading: insights from a 3D lake model. Water Resour. Res. 56, e2019WR027040.

Boedecker, A.R., Niewinski, D.N., Newell, S.E., Chaffin, J.D., McCarthy, M.J., 2020. Evaluating sediments as an ecosystem service in western Lake Erie via quantification of nutrient cycling pathways and selected gene abundances. J. Great Lakes Res. 46, 920–932.

Bolsenga, S.J., Herdendorf, C.E., 1993. Lake Erie and Lake St. Clair Handbook. Wayne State University Press.

Boström, B., Jansson, M., Forsberg, C., 1982. Phosphorus release from lake sediments. Arch. Hydrobiol. Beih. 18, 5–59.

Burniston, D., Dove, A., Backus, S., Thompson, A., 2018. Nutrient concentrations and loadings in the St. Clair River - Detroit River Great Lakes Interconnecting Channel. J. Great Lakes Res. 44, 398–411.

Burns, N.M., 1976. Nutrient budgets for Lake Erie, 1970. J. Fish. Res. Board Can. 33, 520–536.

Burns, N.M., Nriagu, J.O., 1976. Forms of iron and manganese in Lake Erie waters. J. Fish. Res. Board Can. 33, 463–470.

Chan, C.H., Williams, D.J., Neilson, M.A., Harrison, B., Archer, M.L., 2003. Spatial and temporal trends in the concentrations of selected organochlorine pesticides (OCs) and polynuclear aromatic hydrocarbons (PAHs) in Great Lakes basin precipitation, 1986 to 1999. J. Great Lakes Res. 29, 448–459.

Chapra, S.C., 1977. Total phosphorus model for the Great Lakes. J. Environ. Eng. Div. ASCE l03, 147–161.

Chapra, S.C., Dolan, D.M., 2012. Great Lakes total phosphorus revisited: 2. Mass balance modeling. J. Great Lakes Res. 38, 741–754.

Chapra, S.C., Sonzogni, W.C., 1979. Great Lakes total phosphorus budget for the mid 1970s. J. Water Pollut. Control Fed. 51, 2524–2533.

Chapra, S.C., Dolan, D.M., Dove, A., 2016. Mass-balance modeling framework for simulating and managing long-term water quality for the lower Great Lakes. J. Great Lakes Res. 42, 1166–1173.

Chen, M., Ye, T.-R., Krumholz, L.R., Jiang, H.-L., 2014. Temperature and cyanobacterial bloom biomass influence phosphorous cycling in eutrophic Lake sediments. PLoS One 9, e93130.

Chen, M., Ding, S., Chen, X., Sun, Q., Fan, X., Lin, J., Ren, M., Yang, L., Zhang, C., 2018. Mechanisms driving phosphorus release during algal blooms based on hourly changes in iron and phosphorus concentrations in sediments. Water Res. 133, 153–164.

Colborne, S.F., Maguire, T.J., Mayer, B., Nightingale, M., Enns, G.E., Fisk, A.T., Drouillard, K.G., Mohamed, M.N., Weisener, C.G., Wellen, C., Mundle, S.O.C., 2019. Water and sediment as sources of phosphate in aquatic ecosystems: the Detroit River and its role in the Laurentian Great Lakes. Sci. Total Environ. 647, 1594–1603.

Derecki, J.A., 1984. Detroit River, physical and hydraulic characteristics. In: Natl. Oceanogr. Atmos. Adm., Great Lakes Environ. Res. Lab., GLERL Contrib., p. 417.

DFO, 2020. Government of Canada. Division of Fisheries and Oceans Canada (DFO). Tides, Currents, and Water Levels. Tidal and Water Level Stations. Available at. https://tides.gc.ca/en/stations [accessed 2020 Oct 1].

Dolan, D.M., 1993. Point source loadings of phosphorus to Lake Erie: 1986–1990. J. Great Lakes Res. 19, 212–223.

Dolan, D.M., Chapra, S.C., 2012. Great Lakes total phosphorus revisited: 1. Loading analysis and update (1994–2008). J. Great Lakes Res. 38, 730–740.

Dolan, D.M., McGunagle, K.P., 2005. Lake Erie total phosphorus loading analysis and update: 1996–2002. J. Great Lakes Res. 31, 11–22.

DWSD, 2019. Detroit water and sewage department (DWSD). In: 2015 Comprehensive Water Master Plan. TM-13: Water Treatment Plant Needs Assessment Study. Available at. tinyurl.com/3xzpb39d [accessed 2019 Jul 3].

Eadie, B.J., Vanderploeg, H.A., Robbins, J.A., Bell, G.L., 1990. Significance of sediment resuspension and particle settling. In: Large Lakes. Springer, Berlin, Heidelberg, pp. 196–209.

Eadie, B.J., Robbins, J.A., Klump, J.V., Schwab, D.J., Edgington, D.N., 2008. Winter-spring storms and their influence on sediment resuspension, transport, and accumulation patterns in southern Lake Michigan. Oceanography 21, 118–135.

Edlund, M.B., Schottler, S.P., Reavie, E.D., Engstrom, D.R., Baratono, N.G., Leavitt, P.R., Heathcote, A.J., Wilson, B., Paterson, A.M., 2017. Historical phosphorus dynamics in Lake of the Woods (USA–Canada)—does legacy phosphorus still affect the southern basin? Lake Reserv. Manage. 33, 386–402.

Ekholm, P., Malve, O., Kirkkala, T., 1997. Internal and external loading as regulators of nutrient concentrations in the agriculturally loaded Lake Pyhäjärvi (Southwest Finland). Hydrobiologia 345, 3–14.

Fu, W., Primeau, F., Keith Moore, J., Lindsay, K., Randerson, J.T., 2018. Reversal of increasing tropical ocean hypoxia trends with sustained climate warming. Global Biogeochem. Cy. 32, 551–564.

Gibbons, K.J., Bridgeman, T.B., 2020. Effect of temperature on phosphorus flux from anoxic western Lake Erie sediments. Water Res. 182, 116022.

GLC, 2019. Great Lakes Commission (GLC). Great Lakes Regional Water Use Dataset. Available at: https://www.glc.org/work/water-use [accessed 2019 Nov 23].

GLERL, 2020a. The United States National Oceanic and Atmospheric Administration (NOAA). Great Lakes Environmental Research Laboratory (GLERL). Great Lakes Monthly Hydrologic Database. Available at: https://www.glerl.noaa.gov/ [accessed 2020 Oct 12].

GLERL, 2020b. The United States National Oceanic and Atmospheric Administration (NOAA). Great Lakes Environmental Research Laboratory (GLERL) Database. Available at: https://coastwatch.glerl.noaa.gov/ [accessed 2020 Dec 20].

GLIP, 2019. Government of Canada. Great Lakes Water Quality Monitoring and Aquatic Ecosystem Health Data. Available at. tinyurl.com/usvytyss [accessed 2019 Dec 7].

GLNPO, 2020. United States Environmental Protection Agency. Great Lakes National Program Office (GLNPO). Great Lakes Water Quality Monitoring Program managed by GLNPO. Available at: https://tinyurl.com/2p88wa5j [accessed 2020 Dec 20].

Gomez, E., Fillit, M., Ximenes, M.C., Picot, B., 1998. Phosphate mobility at the sediment–water interface of a Mediterranean lagoon (etang du Méjean), seasonal phosphate variation. Hydrobiologia 374, 203–216.

Griffiths, R.W., Thornley, S., Edsall, T.A., 1991. Limnological aspects of the St. Clair River. In: Environmental Assessment and Habitat Evaluation of the Upper Great Lakes Connecting Channels. Springer, Dordrecht, pp. 97–123.

Hecky, R.E., Smith, R.E.H., Barton, D.R., Guildford, S.J., Taylor, W.D., Charlton, M.N., Howell, T., 2004. The nearshore phosphorus shunt: a consequence of ecosystem engineering by dreissenids in the Laurentian Great Lakes. Can. J. Fish. Aquat. Sci. 61, 1285–1294.

Hill, B., Dove, A., 2021. Concentrations and loads of nutrients and major ions in the Niagara River, 1975–2018. J. Great Lakes Res. 47, 844–861.

Hirsch, R.M., Moyer, D.L., Archfield, S.A., 2010. Weighted regression on time, discharge, and season (WRTDS), with an application to Chesapeake Bay river inputs. JAWRA 46, 857–880.

Ho, J.C., Michalak, A.M., 2017. Phytoplankton blooms in Lake Erie impacted by both longterm and springtime phosphorus loading. J. Great Lakes Res. 43, 221–228.

HYDAT, 2020. Government of Canada. National Water Data Archive (HYDAT). Available at. tinyurl.com/526vt95a [accessed 2020 Jan 18].

IJC (International Joint Commission), 1978. Great Lakes Water Quality Agreement of 1978, with annexes and terms of reference, between the United States and Canada. IJC: Windsor, Ontario, Canada, November 22, 1978.

Isles, P.D., Giles, C.D., Gearhart, T.A., Xu, Y., Druschel, G.K., Schroth, A.W., 2015. Dynamic internal drivers of a historically severe cyanobacteria bloom in Lake Champlain revealed through comprehensive monitoring. J. Great Lakes Res. 41, 818–829.

Jabbari, A., Ackerman, J.D., Boegman, L., Zhao, Y., 2019. Episodic hypoxia in the western basin of Lake Erie. Limnol. Oceanogr. 64, 2220–2236.

Jabbari, A., Ackerman, J.D., Boegman, L., Zhao, Y., 2021. Increases in Great Lake winds and extreme events facilitate interbasin coupling and reduce water quality in Lake Erie. Sci. Rep. 11, 5733.

James, W.F., 2017. Internal phosphorus loading contributions from deposited and resuspended sediment to the Lake of the Woods. Lake Reserv. Manage. 33, 347–359.

Janus, L.L., Vollenweider, R.A., 1984. Phosphorus residence time in relation to trophic conditions in lakes. Verh. Internat. Verein. Limnol. 22, 179–184.

Jeppesen, E., Peder Jensen, J., Søndergaard, M., Lauridsen, T., Junge Pedersen, L., Jensen, L., 1997. Top-down control in freshwater lakes: the role of nutrient state, submerged macrophytes and water depth. Hydrobiologia 342, 151–164.

Kemp, A.L.W., MacInnis, G.A., Harper, N.S., 1977. Sedimentation rates and a revised sediment budget for Lake Erie. J. Great Lakes Res. 3, 221–233.

Maccoux, M.J., Dove, A., Backus, S.M., Dolan, D.M., 2016. Total and soluble reactive phosphorus loadings to Lake Erie: a detailed accounting by year, basin, country, and tributary. J. Great Lakes Res. 42, 1151–1165.

Manning, P.G., Birchall, T., Jones, W., 1984. The partitioning of non-apatite inorganic phosphorus in sediments from lakes Erie and Ontario. Can. Mineral. 22, 357–365.

Markelov, I., Couture, R.M., Fischer, R., Haande, S., Van Cappellen, P., 2019. Coupling water column and sediment biogeochemical dynamics: modeling internal phosphorus loading, climate change responses, and mitigation measures in Lake Vansjø, Norway. J. Geophys. Res-Biogeo. 124, 3847–3866.

Matisoff, G., Kaltenberg, E.M., Steely, R.L., Hummel, S.K., Seo, J., Gibbons, K.J., Bridgeman, T.B., Seo, Y., Behbahani, M., James, W.F., Johnson, L.T., 2016. Internal loading of phosphorus in western Lake Erie. J. Great Lakes Res. 42, 775–788.

Matisoff, G., Watson, S.B., Guo, J., Duewiger, A., Steely, R., 2017. Sediment and nutrient distribution and resuspension in Lake Winnipeg. Sci. Total Environ. 575, 173–186.

McKinney, P., Austin, J., Fai, G., 2019. The wind-driven formation of cross-shelf sediment plumes in a large lake. Limnol. Oceanogr. 64, 1309–1322.

Meier, H.M., Andersson, H.C., Eilola, K., Gustafsson, B.G., Kuznetsov, I., Müller-Karulis, B., Neumann, T., Savchuk, O.P., 2011. Hypoxia in future climates: a model ensemble study for the Baltic Sea. Geophys. Res. Lett. 38, L24608.

Mortimer, C.H., 1987. Fifty years of physical investigations and related limnological studies on Lake Erie, 1928–1977. J. Great Lakes Res. 13, 407–435.

Munkes, B., 2005. Eutrophication, phase shift, the delay and the potential return in the Greifswalder Bodden, Baltic Sea. Aquat. Sci. 67, 372–381.

Najjar, R.G., Pyke, C.R., Adams, M.B., Breitburg, D., Hershner, C., Kemp, M., Howarth, R., Mulholland, M.R., Paolisso, M., Secor, D., Sellner, K., 2010. Potential climate-change impacts on the Chesapeake Bay. Estuar. Coast. Shelf S. 86, 1–20.

NCWQR, 2020. National Center for Water Quality Research (NCWQR). Heidelberg Tributary Loading Program (HTLP) Dataset. Zenodo. https://doi.org/10.5281/zenodo.6606949 [accessed 2020 May 10].

NOAA, 2020a. National Oceanic and Atmospheric Administration (NOAA). In: National Centers for Environmental Information (NCEI). Marine Geology and Geophysics. Bathymetry of Lake Erie & Lake Saint Clair. Available at: https://tinyurl.com/yrwxpk9t [accessed 2020 Aug 15].

NOAA, 2020b. National Oceanic and Atmospheric Administration (NOAA). Tides and Currents. Available at: https://tidesandcurrents.noaa.gov/ [accessed 2020 Jul 10].

Nürnberg, G., LaZerte, B., 2015. Water Quality Assessment in the Thames River Watershed–Nutrient and Sediment Sources. The Upper Thames River Conservation Authority, Baysville, Ontario.

Nürnberg, G.K., LaZerte, B.D., 2016. More than 20 years of estimated internal phosphorus loading in polymictic, eutrophic Lake Winnipeg, Manitoba. J. Great Lakes Res. 42, 18–27.

Nürnberg, G.K., Howell, T., Palmer, M., 2019. Long-term impact of Central Basin hypoxia and internal phosphorus loading on north shore water quality in Lake Erie. Inland Waters 9, 362–373.

O'Connell, D.W., Ansems, N., Kukkadapu, R.K., Jaisi, D., Orihel, D.M., Cade-Menun, B.J., Hu, Y., Wiklund, J., Hall, R.I., Chessell, H., Behrends, T., 2020. Changes in sedimentary phosphorus burial following artificial eutrophication of Lake 227, Experimental Lakes Area, Ontario, Canada. J. Geophys. Res-Biogeo 125, 2020JG005713.

ODC, 2019. Ontario Data Catalogue (ODC). Ontario Watershed Boundaries. Available at: https://tinyurl.com/yxnrpldn [accessed 2019 Jan 9].

Orihel, D.M., Baulch, H.M., Casson, N.J., North, R.L., Parsons, C.T., Seckar, D.C., Venkiteswaran, J.J., 2017. Internal phosphorus loading in Canadian fresh waters: a critical review and data analysis. Can. J. Fish. Aquat. Sci. 74, 2005–2029.

Parsons, C.T., Rezanezhad, F., O'Connell, D.W., Van Cappellen, P., 2017. Sediment phosphorus speciation and mobility under dynamic redox conditions. Biogeosciences 14, 3585–3602.

Paytan, A., Roberts, K., Watson, S., Peek, S., Chuang, P.C., Defforey, D., Kendall, C., 2017. Internal loading of phosphate in Lake Erie central basin. Sci. Total Environ. 579, 1356–1365.

PGMN, 2022. Government of Ontario. Ontario Provincial Groundwater Monitoring Network (PGMN). Available at: https://tinyurl.com/7jmzxw5e [accessed 2022 Jul 8].

PWQMN, 2019. Government of Ontario. Data Catalogue. Provincial (Stream) Water Quality Monitoring Network (PWQMN). Available at: www.tinyurl.com/c756n2pc [accessed 2019 Dec 15].

Radosavljevic, J., Slowinski, S., Shafii, M., Akbarzadeh, Z., Rezanezhad, F., Parsons, C.T., Withers, W., Van Cappellen, P., 2022. Salinization as a driver of eutrophication symptoms in an urban Lake (lake Wilcox, Ontario, Canada). Sci. Total Environ. 846, 157336.

Rowe, M.D., Anderson, E.J., Beletsky, D., Stow, C.A., Moegling, S.D., Chaffin, J.D., May, J.C., Collingsworth, P.D., Jabbari, A., Ackerman, J.D., 2019. Coastal upwelling influences hypoxia spatial patterns and nearshore dynamics in Lake Erie. J. Geophys. Res.-Oceans 124, 6154–6175.

Rucinski, D., Scavia, D., DePinto, J., Beletsky, D., 2014. Lake Erie's hypoxia response to nutrient loads and meteorological variability. J. Great Lakes Res. 40, 151–161.

Sabur, M.A., Parsons, C.T., Maavara, T., Van Cappellen, P., 2021. Effects of pH and dissolved silicate on phosphate mineral-water partitioning with goethite. ACS Earth Space Chem. 6, 34–43.

Sayers, M.J., Grimm, A.G., Shuchman, R.A., Bosse, K.R., Fahnenstiel, G.L., Ruberg, S.A., Leshkevich, G.A., 2019. Satellite monitoring of harmful algal blooms in the Western Basin of Lake Erie: a 20-year time-series. J. Great Lakes Res. 45, 508–521.

Scavia, D., Allan, J.D., Arend, K.K., Bartell, S., Beletsky, D., Bosch, N.S., Brandt, S.B., Briland, R.D., Daloğlu, I., DePinto, J.V., Dolan, D.M., Evans, M.A., Farmer, T.M., Goto, D., Han, H., Höök, T.O., Knight, R., Ludsin, S.A., Mason, D., Michalak, A.M., Richards, R.P., Roberts, J.J., Rucinski, D.K., Rutherford, E., Schwab, D.J., Sesterhenn, T., Zhang, H., Zhou, Y., 2014. Assessing and addressing the re-eutrophication of Lake Erie: central basin hypoxia. J. Great Lakes Res. 40, 226–246.

Scavia, D., Bocaniov, S.A., Dagnew, A., Hu, Y., Kerkez, B., Long, C.M., Muenich, R.L., Read, J., Vaccaro, L., Wang, Y.C., 2019a. Detroit River phosphorus loads: anatomy of a binational watershed. J. Great Lakes Res. 45, 1150–1161.

Scavia, D., Bocaniov, S.A., Dagnew, A., Long, C., Wang, Y.C., 2019b. St. Clair-Detroit River system: phosphorus mass balance and implications for Lake Erie load reduction, monitoring, and climate change. J. Great Lakes Res. 45, 40–49.

Scavia, D., Anderson, E.J., Dove, A., Hill, B., Long, C.M., Wang, Y.C., 2020. Lake Huron's phosphorus contributions to the St. Clair–Detroit River Great Lakes connecting channel. Environ. Sci. Technol. 54, 5550–5559.

Scavia, D., Wang, Y.-C., Obenour, D.R., Apostel, A., Basile, S.J., Kalcic, M.M., Kirchhoff, C.J., Miralha, L., Muenich, R.L., Steiner, A.L., 2021. Quantifying uncertainty cascading from climate, watershed, and lake models in harmful algal bloom predictions. Sci. Total Environ. 759, 143487.

Scavia, D., Calappi, T.J., Godwin, C.M., Hill, B., Veliz, M., Wang, Y.-C., 2022. Wind-driven sediment resuspension in the world's fourth-largest lake contributes a substantial phosphorus load to the eleventh-largest lake. Environ. Sci. Technol. 56, 11061–11070.

Scavia, D., Wang, Y.-C., Obenour, D.R., 2023. Advancing freshwater ecological forecasts: harmful algal blooms in Lake Erie. Sci. Total Environ. 856, 158959.

Søndergaard, M., Jensen, J.P., Jeppesen, E., 2003. Role of sediment and internal loading of phosphorus in shallow lakes. Hydrobiologia 506, 135–145.

Sonzogni, W.C., Uttormark, P.C., Lee, G.F., 1976. The phosphorus residence time model: theory and application. Water Res. 10, 429–435.

Soranno, P.A., Carpenter, S.R., Lathrop, R.C., 1997. Internal phosphorus loading in Lake Mendota: response to external loads and weather. Can. J. Fish. Aquat. Sci. 54, 1883–1893.

Stigebrandt, A., Andersson, A., 2020. The eutrophication of the Baltic Sea has been boosted and perpetuated by a major internal phosphorus source. Front. Mar. Sci. 7, 572994.

Stone, M., Saunderson, H., 1992. Particle size characteristics of suspended sediment in southern Ontario rivers tributary to the Great Lakes. Hydrol. Process. 6, 189–198.

Stone, M., Saunderson, H.C., 1996. Regional patterns of sediment yield in the Laurentian Great Lakes basin. In: Walling, D.E., Webb, B.W. (Eds.), Erosion and Sediment Yield, Global and Regional Perspectives (Proceedings of the Exeter Symposium, July 1996), 236. IAHS Publ., pp. 125–131

Stumpf, R.P., Johnson, L.T., Wynne, T.T., Baker, D.B., 2016. Forecasting annual cyanobacterial bloom biomass to inform management decisions in Lake Erie. J. Great Lakes Res. 42, 1174–1183.

Tammeorg, O., Nürnberg, G.K., Tõnno, I., Kisand, A., Tuvikene, L., Nõges, T., Nõges, P., 2022. Sediment phosphorus mobility in Võrtsjärv, a large shallow lake: insights from phosphorus sorption experiments and long-term monitoring. Sci. Total Environ. 829, 154572.

Thomas, R.L., Christensen, M.D., Szalinska, E., Scarlat, M., 2006. Formation of the St. Clair River Delta in the Laurentian Great Lakes system. J. Great Lakes Res. 32, 738–748.

USGS, 2019. The United States Geological Service (USGS). National Water Information System. Available at: https://waterdata.usgs.gov/nwis [accessed 2019 Dec 20].

USGS, 2022. The United States Geological Service (USGS). National Ground-Water Monitoring Network (NGWMN) Data Portal. Available at: https://cida.usgs.gov/ngwmn/ [accessed 2022 Aug 29].

Vahtera, E., Conley, D.J., Gustafsson, B.G., Kuosa, H., Pitkänen, H., Savchuk, O.P., Tamminen, T., Viitasalo, M., Voss, M., Wasmund, N., Wulff, F., 2007. Internal ecosystem feedbacks enhance nitrogen-fixing cyanobacteria blooms and complicate management in the Baltic Sea. Ambio 36, 186–194.

Wang, Y.T., Zhang, T.Q., Zhao, Y.C., Ciborowski, J.J.H., Zhao, Y.M., O'Halloran, I.P., Qi, Z.M., Tan, C.S., 2021. Characterization of sedimentary phosphorus in Lake Erie and on-site quantification of internal phosphorus loading. Water Res. 188, 116525.

Watson, S.B., Miller, C., Arhonditsis, G., Boyer, G.L., Carmichael, W., Charlton, M.N., Confesor, R., Depew, D.C., Höök, T.O., Ludsin, S.A., Matisoff, G., 2016. The re-eutrophication of Lake Erie: harmful algal blooms and hypoxia. Harmful Algae 56, 44–66.

WBD, 2019. The United States Geological Survey (USGS). Watershed Boundary Dataset (WBD). Available at. https://tinyurl.com/y6flcn4g [accessed 2019 Nov 1].

Welch, E.B., Cooke, G.D., 1995. Internal phosphorus loading in shallow lakes: importance and control. Lake Reserv. Manage. 11, 273–281.

Williams, J.D.H., Jaquet, J.M., Thomas, R.L., 1976. Forms of phosphorus in the surficial sediments of Lake Erie. J. Fish. Res. Board Can. 33, 413–429.

Wood, S.N., 2011. Fast stable restricted maximum likelihood and marginal likelihood estimation of semiparametric generalized linear models. J. R. Stat. Soc. Ser. B 73, 3–36.

Wood, S.N., 2017. Generalized Additive Models: An Introduction with R, 2nd ed. Chapman and Hall/CRC.

WQMSD, 2019. Government of Canada. Environment and Climate Change Canada (ECCC). Great Lakes Water Quality Monitoring and Surveillance Data (WQMSD). Burlington, Ontario, Canada.

WQP, 2019. The Water Quality Portal (WQP). A cooperative service sponsored by the United States Geological Survey (USGS), the Environmental Protection Agency (EPA), and the National Water Quality Monitoring Council (NWQMC). Available at. https://www.waterqualitydata.us/ [accessed 2019 Dec 3].

Xu, S., Frey, S.K., Erler, A.R., Khader, O., Berg, S.J., Hwang, H.T., Callaghan, M.V., Davison, J.H., Sudicky, E.A., 2021. Investigating groundwater-lake interactions in the Laurentian Great Lakes with a fully-integrated surface water-groundwater model. J. Hydrol. 594, 125911.

Yang, C., Yang, P., Geng, J., Yin, H., Chen, K., 2020. Sediment internal nutrient loading in the most polluted area of a shallow eutrophic lake (Lake Chaohu, China) and its contribution to lake eutrophication. Environ. Pollut. 262, 114292.

Zepernick, B.N., Gann, E.R., Martin, R.M., Pound, H.L., Krausfeldt, L.E., Chaffin, J.D., Wilhelm, S.W., 2021. Elevated pH conditions associated with Microcystis spp. blooms decrease viability of the cultured diatom *Fragilaria crotonensis* and natural diatoms in Lake Erie. Front. Microbiol. 12, 598736.

Zhou, Y., Obenour, D.R., Scavia, D., Johengen, T.H., Michalak, A.M., 2013. Spatial and temporal trends in Lake Erie hypoxia, 1987–2007. Environ. Sci. Technol. 47, 899–905.